Dalton Transactions

Cite this: *Dalton Trans.*, 2012, **41**, 13862

www.rsc.org/dalton

PAPER

Acyloxybutadiene tricarbonyl iron complexes as enzyme-triggered CO-releasing molecules (ET-CORMs): a structure–activity relationship study†

Steffen Romanski,[a] Birgit Kraus,[b] Miguel Guttentag,[c] Waldemar Schlundt,[a] Hannelore Rücker,[d] Andreas Adler,[a] Jörg-Martin Neudörfl,[a] Roger Alberto,[c] Sabine Amslinger*[d] and Hans-Günther Schmalz*[a]

Received 22nd March 2012, Accepted 14th May 2012
DOI: 10.1039/c2dt30662j

A series of η^4-acyloxycyclohexadiene–$Fe(CO)_3$ complexes was prepared and fully characterized by spectroscopic methods including single crystal X-ray diffraction. For this purpose a new synthetic access to differently acylated 1,3- and 1,5-dienol–$Fe(CO)_3$ complexes was developed. The enzymatically triggered CO release from these compounds was monitored (detection of CO through GC and/or by means of a myoglobin assay) and the anti-inflammatory effect of the compounds was assessed by a cellular assay based on the inhibition of NO-production by inducible NO synthase (iNOS). It was demonstrated that the properties (rate of esterase-triggered CO release, iNOS inhibition, cytotoxicity) of the complexes strongly depend on the substitution pattern of the π-ligand and the nature of the acyloxy substituent.

Introduction

Carbon monoxide (CO) has recently been recognized as an important signalling molecule in mammals.[1] Most of the endogenously produced CO is generated in the course of oxidative heme degradation by the heme oxygenase (HO) enzymes. One of the isoforms of these enzymes (HO-1) is inducible and up-regulated as a response to stress.[2] CO induces several beneficial biological effects, such as cytoprotection, vasodilation, or inhibition of inflammation,[3] and there are clinical studies on different medical applications.[4] One attractive option to deliver CO (avoiding the use of toxic CO gas) is the use of CO-releasing molecules (CORMs).[5] Motterlini and co-workers established this constantly growing field by the identification and evaluation of certain transition metal carbonyl complexes, such as $[Mn_2(CO)_{10}]$ (CORM-1), fulfilling this function.[6] Later, compounds with improved properties were developed. A prominent example is *fac*-[RuCl(glycinato)$(CO)_3$] (**1**, CORM-3),[7] a water soluble complex that releases CO under physiological conditions and is undoubtedly the most studied CORM (Fig. 1).[8] While a number of different CORMs were shown to exhibit promising activities in various biological investigations,[9] an important unsolved challenge is the delivery of controlled amounts of CO to a target tissue. A general strategy to achieve this aim is the use of stable molecules, which release CO only after activation by means of a trigger.[10] Two possibilities are (1) the pH-dependent CO release from boranocarbonate (**2**, CORM-A1)[11] or amino-derivatives thereof,[12] or (2) the UV-triggered CO release from transition metal carbonyl complexes.[13]

As a novel concept, we recently introduced acyloxybutadiene–$Fe(CO)_3$ complexes of type **3** as enzyme-triggered CO-releasing molecules (ET-CORMs).[14] The earlier observation, that enol complexes of type **4** are labile and decompose under oxidative conditions, suggested their suitability as CORMs (Scheme 1). As stable (and "storable") precursors we devised the corresponding esters, *i.e.* acyloxydiene complexes of type **3**, which are sufficiently stable under physiological conditions but are readily converted to the "active" species **4** by means of enzymatic hydrolysis. Thus, once a complex of type **3** enters a cell, cleavage of the ester function by an intracellular esterase triggers the desired CO-release by generating the labile enol complex **4**. The oxidative decomposition of this type of intermediate (presumably *via* a 16-VE species of type **5**) leads to the liberation of the enone ligand and to the release of three molecules of CO (Scheme 1).

1 (CORM 3) **2** (CORM A1)

Fig. 1 Structures of CORM-3 (**1**) and CORM A1 (**2**).

[a]*Department für Chemie, Universität zu Köln, 50937 Köln, Germany. E-mail: schmalz@uni-koeln.de*
[b]*Lehrstuhl für Pharmazeutische Biologie, Universität Regensburg, 93053 Regensburg, Germany*
[c]*Institut für Anorganische Chemie, Universität Zürich, CH-8057 Zürich, Switzerland*
[d]*Institut für Organische Chemie, Universität Regensburg, 93503 Regensburg, Germany. E-mail: sabine.amslinger@chemie.uni-regensburg.de*

†Electronic supplementary information (ESI) available: Full experimental and spectroscopic data of all compounds. Detailed description of CO-releasing experiments, Crystallographic Data. CCDC 872868–872874. For ESI and crystallographic data in CIF or other electronic format see DOI: 10.1039/c2dt30662j

In our initial study we succeeded in proving the concept, *i.e.* the enzyme-triggered CO-release from compounds of type **3**, by synthesis and evaluation of complexes *rac*-**6**, *rac*-**7**, *rac*-**8** and *rac*-**9** (Scheme 2, inner circle). These compounds showed very promising effects in a cellular assay based on the inhibition of NO-production by inducible NO-synthase (iNOS). Moreover, a strong dependency of the reactivity (towards enzymatic ester hydrolysis) and the biological activity on the structure of the complexes was observed. These interesting results prompted us to further explore this class of compounds. We here disclose the results of a much more detailed study, which has led to the identification of pronounced structure–activity relationships.

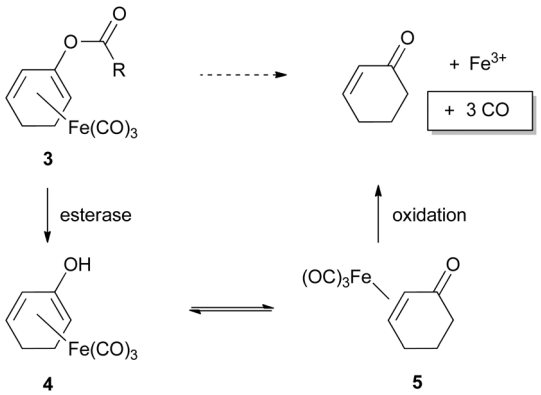

Scheme 1 Proposed mechanism of action of enzyme-triggered CO-releasing molecules (ET-CORMs) of type **3**.

Results and discussion

Synthesis

The various acyloxydiene–$Fe(CO)_3$ complexes used in the present study are displayed in Fig. 2. Compounds *rac*-**6**, *rac*-**7** and *rac*-**8** were synthesized as described before.[14] Di-acetates *rac*-**9** and *rac*-**16** were prepared using a slightly modified version of the Boháč procedure.[15] Complex *rac*-**10** was synthesized from cyclohexenone (**19**) by deprotonation with LiHMDS in the presence of TPPA (2.5 equiv.) followed by *O*-acylation of the resulting dienolate with pivaloyl chloride (PivCl). The resulting dienyl pivalate **20** was treated with $Fe_2(CO)_9$ in refluxing diethyl

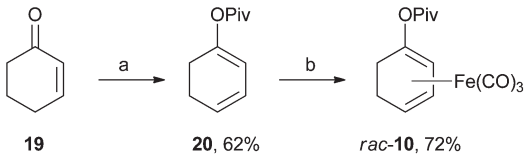

Scheme 2 Synthesis of complex *rac*-**10**. (a) LiHMDS, TPPA, THF, −78 °C, then PivCl; (b) $Fe_2(CO)_9$, Et_2O, 40 °C, 16 h. LiHMDS: lithium hexamethyldisilazide; PivCl: pivaloyl chloride; TPPA: trispyrrolidino phosphoric acid triamide.

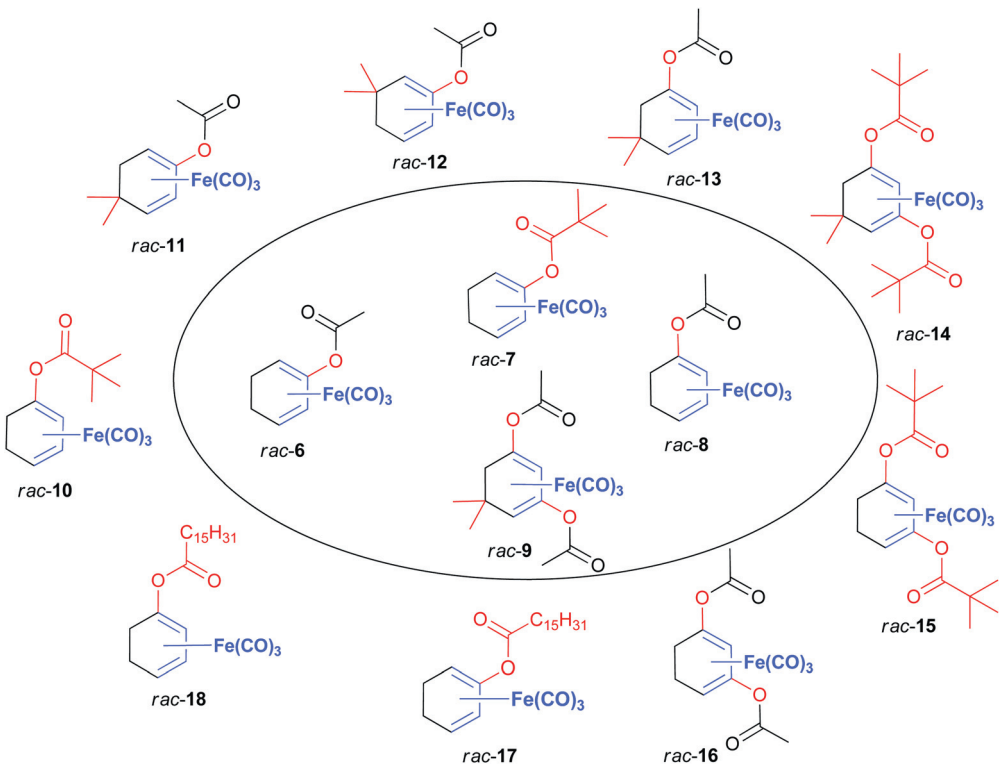

Fig. 2 Acyloxydiene–$Fe(CO)_3$ complexes used in this study as potential ET-CORMs for the evaluation of structure–activity relationships. Compounds *rac*-**6**, *rac*-**7**, *rac*-**8** and *rac*-**9** were reported in our previous study.[14] The focus of this study is the variation of the structural elements marked in red, *i.e.* the type of the ester group and additional methyl substituents at the cyclohexene ring.

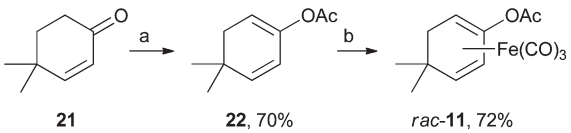

Scheme 3 (a) LDA, THF, −78 °C, then Ac_2O; (b) $Fe_2(CO)_9$, Et_2O, 40 °C, 16 h. LDA: lithium diisopropyl amide.

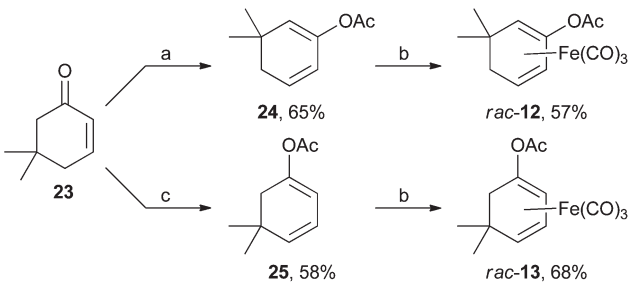

Scheme 4 (a) LDA, THF, −78 °C, then Ac_2O; (b) $Fe_2(CO)_9$, Et_2O, 40 °C, 16 h; (c) LiHMDS, TPPA, THF, −78 °C, then Ac_2O.

ether to generate the desired complex *rac*-**10** in good yield (Scheme 2).

The three complexes *rac*-**11**, *rac*-**12** and *rac*-**13** were synthesized in a similar manner, starting from different cyclohexenones. Compound *rac*-**11** was prepared starting from 4,4-dimethylcyclohexenone (**21**)[16] by deprotonation with LDA and trapping of the resulting dienolate with Ac_2O. Complexation of the resulting dienyl acetate **22** then afforded *rac*-**11** (Scheme 3).

Complexes *rac*-**12** and *rac*-**13** were synthesized from 5,5-dimethylcyclohexenone (**23**), which was obtained from dimedone (**27**) using the two-step protocol of Wawrzénczyk and Lochyński.[17] Regioselective deprotonation of **23** under either kinetic (LDA, THF) or thermodynamic (LiHMDS, TPPA)[14] control, subsequent *O*-acetylation and final complexation led to *rac*-**12** and *rac*-**13**, respectively, as pure isomers after chromatography (Scheme 4).

The complexes *rac*-**14** and *rac*-**15** were readily obtained from the 1,3-diketones **26** or **27** in a three-step procedure. At first, the β-pivaloxy-substituted enones (vinylogous anhydrides) **28** and **29**, respectively, were prepared. Subsequent deprotonation with LDA, *O*-pivaloylation of the enolate intermediates and complexation then afforded the desired products (Scheme 5).[18]

An attempt to apply a related protocol to the synthesis of the dienyl palmitate complexes *rac*-**17** and *rac*-**18** failed, because we could not achieve the synthesis of the dienyl palmitates (as complexation precursors). The problem was solved (according to the strategy of Yeh and Hwu)[19] by first preparing a siloxy-substituted complex (*rac*-**34**/**35**) and subsequently replacing the silyl by an acyl unit (Scheme 6). The siloxydiene **32** was obtained from **19** with LDA and TMSCl. Subsequent complexation afforded *rac*-**34** which, without isolation, was deprotected by chromatography on SiO_2 under inert conditions (N_2) to give the dienol complex *rac*-**36**. This sensitive compound was immediately converted to the desired ester *rac*-**17** with NaH and the acid chloride. A drawback of this sequence is the low yield (and low reproducibility) resulting from the necessity to isolate the highly labile intermediate *rac*-**36**, which is a compound of type **4**.

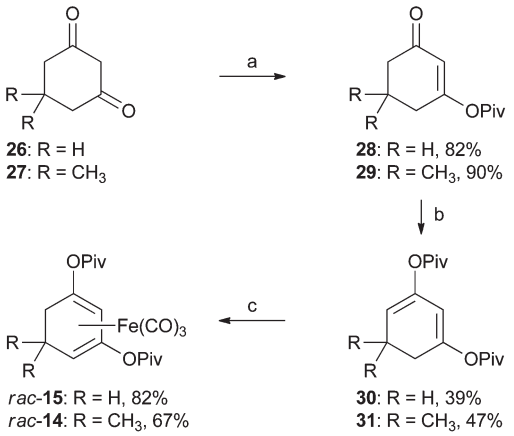

Scheme 5 (a) Pyridine, DCM, 20 °C, then PivCl; (b) LDA, THF, −78 °C, then Ac_2O; (c) $Fe_2(CO)_9$, Et_2O, 40 °C, 16 h.

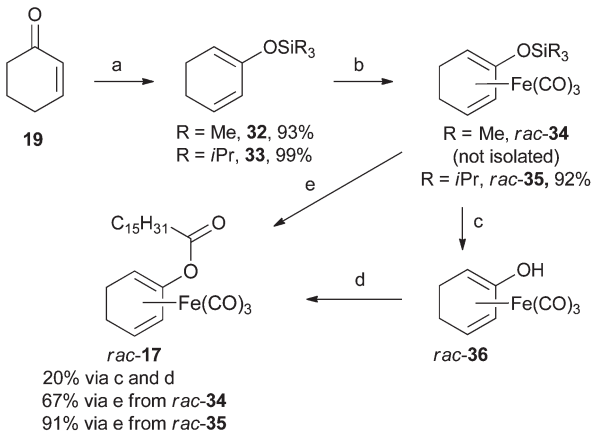

Scheme 6 (a) LDA, THF, −78 °C, then TMSCl or TIPSOTf; (b) $Fe_2(CO)_9$, Et_2O, 40 °C, 16 h; (c) SiO_2, inert conditions; (d) NaH, DMF, 0 °C, then $C_{15}H_{31}COCl$; (e) NaH, DMF, TBAF, 0 °C, then $C_{15}H_{31}COCl$. TIPSOTf: triisopropylsilyl trifluoromethanesulfonate; TBAF: tetra-*n*-butyl ammonium fluoride.

To overcome this disadvantage we deprotected the raw complexation product (*rac*-**34**) by addition of TBAF and reacted the *in situ*-formed dienol complex directly with NaH and the acid chloride. This way, the desired complex *rac*-**17** was obtained with an improved yield and good reproducibility. Using the TIPS-derivative **33**, the siloxy-substituted diene complex *rac*-**34** was stable enough to be purified by chromatography and *rac*-**17** was obtained in a greatly improved overall yield (Scheme 6).

The synthesis of the isomeric compound *rac*-**18** was achieved by applying a related methodology (Scheme 7). The TMS-protected diene, *i.e.* (cyclohexa-1,3-dien-1-yloxy)trimethylsilane, was not synthesized, but the corresponding more stable TIPS derivative **37** (obtained from **19** with LiHMDS/TPPA and TIPSOTf) allowed us to prepare the siloxydiene complex *rac*-**38** in excellent yield. Deprotection with TBAF and trapping of the resulting di-enolate complex with palmitoyl chloride in the presence of a base (NaH or DIPEA) gave rise to *rac*-**18** in high yield (Scheme 7).

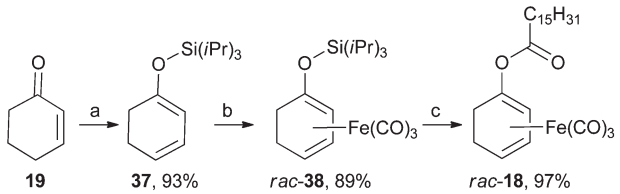

Scheme 7 (a) LiHMDS, TPPA, THF, −78 °C, then TIPSOTf; (b) $Fe_2(CO)_9$, Et_2O, 40 °C, 16 h; (c) TBAF, DIPEA, DMF, 20 °C, then $C_{15}H_{31}COCl$. DIPEA: diisopropylethylamine.

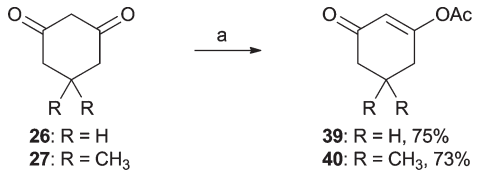

Scheme 8 (a) Pyridine, DCM, 20 °C, then AcCl.

To evaluate also the biological activity of the expected organic by-products of the particularly active ET-CORMs (*rac*-**9** and *rac*-**16**), the enones **39** and **40** were required as reference substances. These compounds were prepared from the diketones **26** and **27**[20] by reaction with AcCl in the presence of pyridine (Scheme 8).

X-Ray diffraction and analytics

All of the prepared acyloxydiene–$Fe(CO)_3$ complexes (Fig. 2) proved to be reasonably air-stable and were fully characterized by the common spectroscopic methods. The structures of the complexes *rac*-**10**, *rac*-**11**, *rac*-**12**, *rac*-**14**, rac-**15**, *rac*-**17** and *rac*-**18** were additionally confirmed by X-ray crystal structure analysis (Fig. 3).

The different positions of the ester substituents, the additional methyl substituents and the different acyl groups did not induce any significant change of the boat-type conformation or the bond lengths within the cyclohexadiene ring. In all cases, the diene moiety of the molecules is virtually planar, with C–C–C–C torsion angles of 0.2–3.6°. The $Fe(CO)_3$ tripod adopts a conformation with one CO ligand eclipsing the Csp^3–Csp^3 single bond. The molecular structures are depicted in Fig. 3. For the X-ray crystallographic data and structural details, see Table 4 and the ESI.†

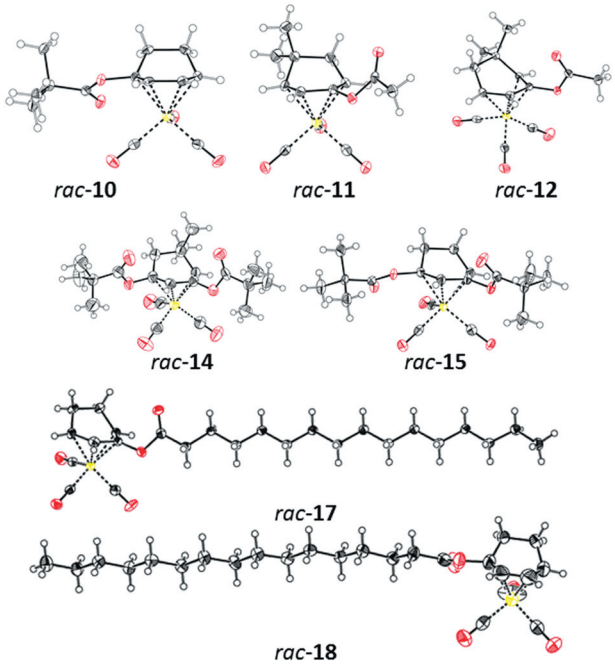

Fig. 3 Molecular structures of *rac*-**10**, *rac*-**11**, *rac*-**12**, *rac*-**14**, *rac*-**15**, *rac*-**17** and *rac*-**18** in the crystalline state. Ellipsoids are drawn at the 50% probability level.

Table 1 Identification of suitable esterases (PLE or LCR) for the cleavage of various acyloxydiene–$Fe(CO)_3$ complexes

Substrate	PLE (high purity)	LCR	PLE (low purity)
rac-**6**	$-^a$	$+^a$	$+^c$
rac-**7**	$-^a$	$\pm^a$	$+^c$
rac-**8**	$+^a$	$+^a$	$+^c$
rac-**9**	$+^a$	$-^a$	$+^c$
rac-**10**	$+^a$	$-^a$	$+^c$
rac-**11**	$-^a$	$+^a$	$+^c$
rac-**12**	$-^a$	$-^a$	$+^c$
rac-**13**	$+^a$	$+^a$	$+^c$
rac-**14**	$+^b$	$-^b$	$+^c$
rac-**15**	$+^b$	$-^b$	$+^c$
rac-**16**	$+^a$	$\pm^a$	$+^c$
rac-**17**	$-^b$	$\pm^{b,c}$	$-^c$
rac-**18**	$+^b$	$+^c$	$+^c$

Conversion was detected as follows: [a] By measuring the kinetic resolution by GC or HPLC on a chiral stationary phase. [b] By detecting the CO-release by means of the Mb-assay. [c] By detecting the CO-release through GC. PLE: pig liver esterase; LCR: lipase from *Candida rugosa*.

Detection of the CO-release

Prior to the *in vitro* evaluation of the CO-releasing properties of the various iron complexes, we had to identify suitable esterases for the enzymatic hydrolysis. In the course of our previous study, pig liver esterase (PLE) and lipase from *Candida rugosa* (LCR) had proved to be most suitable (out of several commercial esterases initially screened). For this reason we investigated the hydrolysis of the different complexes using these enzymes. The kinetic resolution of the (racemic) compounds was taken as unambiguous proof of enzymatic hydrolysis. For this purpose the enantiomeric excess of the remaining complex was determined by means of HPLC or GC on a chiral stationary phase. In some cases (*rac*-**14**, *rac*-**15**, *rac*-**17** and *rac*-**18**) no sufficient enantiomer separation was achieved. In these cases we used the CO-release, as determined by the myoglobin (Mb) assay or GC (see below), as an indirect method to prove the enzymatic cleavage.[21] Noteworthy, PLE of high purity (130 U mg^{-1}) was required for the Mb assay to prevent Mb degradation by protease impurities. Nevertheless, these impurities of the cheaper PLE (15 U mg^{-1}) proved to be beneficial for the hydrolysis of certain complexes (monitored by GC detection of the CO release). The results of the various hydrolysis experiments are summarized in Table 1.

Table 2 Quantification of CO-release in the monitored period and times for the release of 0.5 mol of CO ($t_{0.5}$) per mol of ET-CORM are given

Complex	Enzyme	Released CO (equiv.)[a]	Time (min)[b]	$t_{0.5}$ (min)
rac-**6**	LCR	2.4	10 020 n.f.	128
rac-**6**	PLE	2.2	5638 n.f.	43
rac-**11**	PLE	0.1	1877 n.f.	—
rac-**12**	PLE	1.0	3444 n.f.	133
rac-**7**	PLE	0.3	4778 n.f.	—
rac-**17**	LCR	0.6	7200 n.f.	6119
rac-**8**	PLE	2.4	300 n.f.	21
rac-**10**	PLE	2.6	2178	28
rac-**13**	PLE	3.1	3300	25
rac-**18**	PLE	1.3	1400	108
rac-**16**	PLE	2.1	600	10
rac-**9**	PLE	3.0	600	5
rac-**15**	PLE	2.3	4320 n.f.	51
rac-**14**	PLE	1.7	4320 n.f.	478

[a] The determination of the absolute amount of CO was complicated by the consumption of oxygen, which varied for the individual compounds (but always stayed in the same range). The average consumption of oxygen was considered in the calibration, but deviations in the range of ±0.2 equiv. cannot be excluded. [b] In cases where the CO release still proceeded when the detection was stopped, "n.f." (not finished) is added as a suffix.

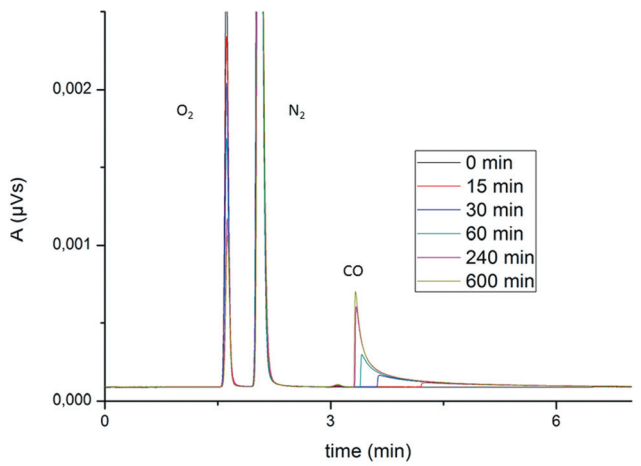

Fig. 4 Monitoring the CO release from *rac*-**9** as a function of the time. The O_2 peak (left) clearly decreases while the CO peak (right) increases.

The esterase-triggered CO-release from the compounds was detected, but not quantified, using the myoglobin (Mb)-based assay established by Motterlini *et al.*[6] To obtain more precise information on the (relative) rates and the quantities of released CO, the enzyme-triggered CO-release of complexes *rac*-**6** to *rac*-**18** was additionally monitored by GC.[22] The times for the release of 0.5 mol of CO per mol of ET-CORM ($t_{0.5}$)[23] from the different complexes under standard conditions (with the specified enzyme) are listed in Table 2. In agreement with the proposed chemical mechanism (Scheme 1), the enzyme-triggered CO release from the acyloxydiene–$Fe(CO)_3$ complexes was found to be associated with a consumption of oxygen in the reaction system, as indicated by a decrease of the O_2 peak connected to the growth of the CO peak (Fig. 4).

As a consequence, the calibration of the GC measurements to quantify the amount of CO formed required particular effort (see ESI†). The results shown in Table 2 reveal the following trends. (1) The CO release from the pivalates and palmitates, respectively, was slower (as compared to the acetates) which corresponds to the expected slower rates of (also enzymatic) hydrolysis.[24] (2) The CO release from the complexes with an ester function at the outer position of the diene (*rac*-**8**, *rac*-**10** and *rac*-**18**) was much faster than the CO release from the complexes with the ester function at the inner position (*rac*-**6**, *rac*-**7** and *rac*-**17**).

This effect results either from a slower rate of ester hydrolysis (dependent on the enzyme used), a lower stability (faster oxidative decay) of the resulting enol intermediates (related to **4**), or a combined effect. (3) The CO release from the diacetate complexes proved to be the fastest. This might be caused by a faster ester hydrolysis or a lower stability of the initially formed enol complex. It also cannot be excluded that hydrolysis of the second ester function triggers an accelerated CO release.

Biological activity

The inducible form of NO-synthase (iNOS) is a dimeric heme protein whose action leads to the formation of NO and L-citrulline from L-arginine in the presence of O_2 and NADPH.[25] The NO released by mammalian cells is employed against invaders such as viruses, bacteria and parasites as well as tumor growth.[26] The influence of CO on the activity of the pro-inflammatory enzyme iNOS can be either on the transcriptional level or on the protein level (Fig. 5). On the transcriptional level, different mechanisms come into play where the activation of the transcription factor nuclear factor-κB (NF-κB)[27] can be inhibited and thus the expression of iNOS. All three decomposition products of ET-CORMs, Fe^{3+} ions[28] and CO[29] as well as the corresponding enones such as cyclohexenone,[30] have been reported to attenuate iNOS protein levels. Enones are of importance since they interfere with the thiol-regulated activation of NF-κB through Michael additions.[31] On the protein level, the enzyme activity of iNOS can be blocked with CO by either inhibiting the formation of the active dimeric form[29] of iNOS or binding of CO to the iron center of the heme prosthetic group.[32] This leads to the deterioration of its catalytic activity to produce NO (Fig. 5). Therefore, the ET-CORMs can act in different ways when inhibiting the production of NO by iNOS. Both their ability to release CO and their decomposition products (*i.e.* the corresponding enones and Fe^{3+}) or a combination thereof may be responsible for the observed activity of the ET-CORMs. That is also true for potential toxic effects, which may additionally be attributed to the complexes themselves.

The biological activity of the ET-CORMs was assessed (using the murine macrophage cell line RAW264.7) by determining their influence on (1) the lipopolysaccharide (LPS)-induced production of NO by iNOS and (2) the cell viability (Table 3). The latter was determined by means of the MTT assay and crystal violet staining, while the inhibition of NO-production was analyzed by the Griess assay.

An overview of the results (including our previous results[14]) is given in Table 3. For a more detailed presentation of the data, see Fig. 6 and the ESI.†

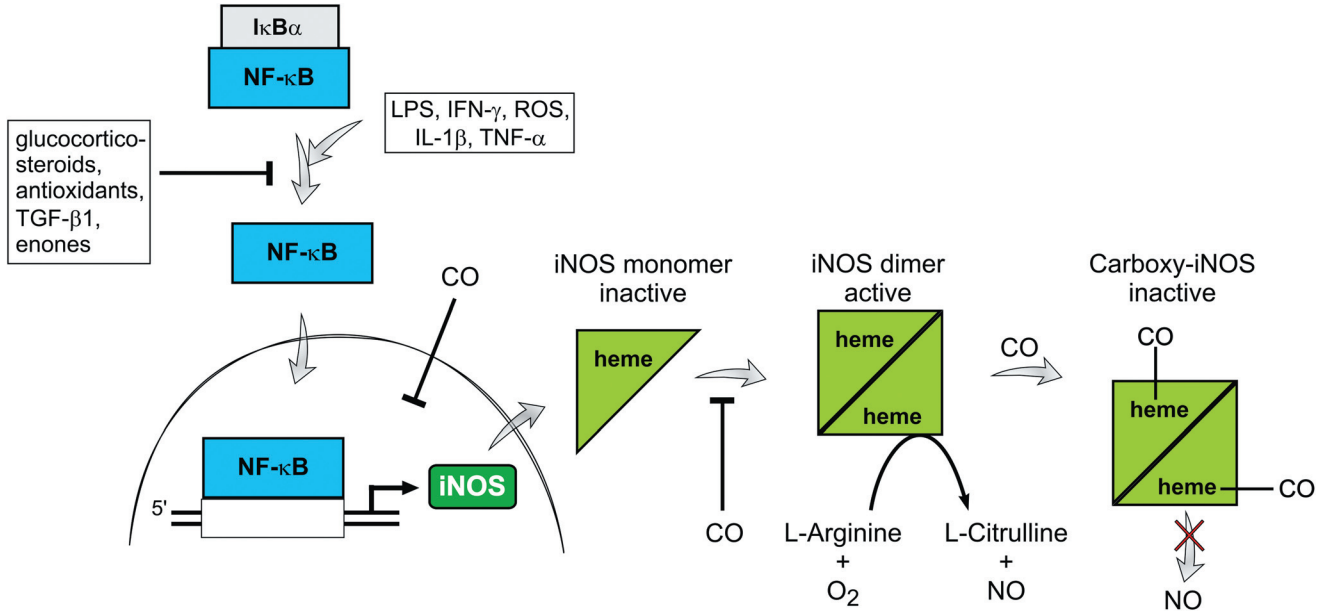

Fig. 5 Potential influences of CORMs on the transcription and protein activity of inducible NO-synthase (iNOS).[25] Inducers of transcription: LPS, lipopolysaccharide; IFN-γ, interferon-γ; ROS, reactive oxygen species/oxidative stress; IL-1β, interleukin-1β; TNF-α, tumor necrosis factor-α. Inhibitors of transcription (= inhibitors of nuclear factor-κB (NF-κB) activation): glucocorticosteroids, antioxidants, transforming growth factor-β1 (TGF-β1) or enones. IκBα, NF-κB inhibitor α.

Table 3 Biological activities of ET-CORMs: cytotoxicity data were determined by MTT or crystal violet assay, and inhibition of NO-production in LPS-stimulated RAW264.7 murine macrophages by Griess assay

	MTT or crystal violet*		Inhibition of NO-production (%)		
Compound	IC_{50} (μM)	IC_{20} (μM)	Minimum (conc (μM))	Maximum (conc (μM))	At 10 μM
rac-**6**	67[a]	28[a]	17 (25)[a]	17 (25)[a]	[a,b]
rac-**7**	>100*[a]	>100*[a]	—[a]	—[a]	—[a]
rac-**8**	40[a]	11[a]	5 (0.5)[a]	49 (10)[a]	49[a]
rac-**9**	54[a]	22[a]	33 (5)[a]	66 (20)[a]	57[a]
rac-**10**	>100	57	11 (10)	23 (50)	11
rac-**11**	41	11	11 (10)	11 (10)	11
rac-**12**	49	18	9 (5)	17 (10)	17
rac-**13**	>100	>100	19 (5)	79 (100)	33
rac-**14**	52	17	—	—	[b]
rac-**15**	69*	25*	16 (15)	42 (25)	[b]
rac-**16**	35	5	8 (1)	34 (5)	[c]
rac-**17**	>100	49	—	—	[b]
rac-**18**	90	31	—	—	[b]
19	62	20	12 (1)	60 (20)	55
23	>100	>100	18 (5)	83 (100)	37
39	>100	>100	12 (50)	15 (100)	[b]
40	>100	>100	6 (10)	9 (100)	6

Significant minimum and maximum NO-inhibition values are given at concentrations that had no toxic effects. *An unusual color was observed with *rac*-**7** and *rac*-**15** in the MTT assay prohibiting a correct assessment of the cell viability, therefore a cell count was done *via* the crystal violet assay. [a] Values taken from ref. 14. [b] No significant inhibition was observed at this concentration. [c] No inhibition could be assigned due to toxicity at this concentration.

The data given in Table 3 immediately reveal compounds *rac*-**8**, *rac*-**9**, *rac*-**13**, *rac*-**15**, and *rac*-**16** as being most promising. Interestingly, diacetates *rac*-**9** and *rac*-**16**, which differ structurally only by the two additional methyl groups in the 5-position of the cyclohexadiene ring (in *rac*-**16**), show a similar reduction of NO-formation at 5 μM (about 34%). However, complex *rac*-**16** is already active at 1.0 μM (7.7%) but due to its toxicity no measurements were performed at concentrations above 5 μM. The less toxic compound *rac*-**9** reduced the NO-production at concentrations ≥5.0 μM, and exhibited a remarkable maximum effect of 66% NO-inhibition at 20 μM (the highest non-toxic concentration). The "outer" monoacetate *rac*-**8** also displayed good inhibition of NO production (49% at 10 μM) but proved again to be more toxic than its dimethylated analog *rac*-**13**, which showed a particularly clear concentration dependency of its iNOS-inhibiting effect (Fig. 6C). The dipivalate *rac*-**15** was less toxic than the corresponding diacetate (*rac*-**16**) but also significantly less active. However, because of the lower toxicity a higher maximum inhibition could be reached (42% at 25 μM). Nevertheless, the most significant inhibition of NO-production was reached with compound *rac*-**13** (79% at 100 μM) as a consequence of its exceptionally low toxicity.

To probe whether the observed activity is merely an effect of CO and cannot be attributed to the enone decomposition products, we also tested the enones **19**, **23**, **39**, and **40** (Fig. 7) for their toxicity and influence on NO-production with LPS-stimulated mouse macrophages.

Enone **39** is not toxic and no NO-inhibition activity was found in the concentration range (1.0–5.0 μM) used for the assessment of *rac*-**16** (Fig. 6E). Therefore, the NO-inhibition caused by *rac*-**16** must be attributed to the CO release. A similar outcome was obtained for *rac*-**9** and its decomposition product, *i.e.* the enone **40**. However, a completely different situation was observed for the mono-acetoxy-substituted complex *rac*-**13** bearing two geminal methyl groups. In this case, both *rac*-**13** and its parent enone **23** possess no toxicity but show a very

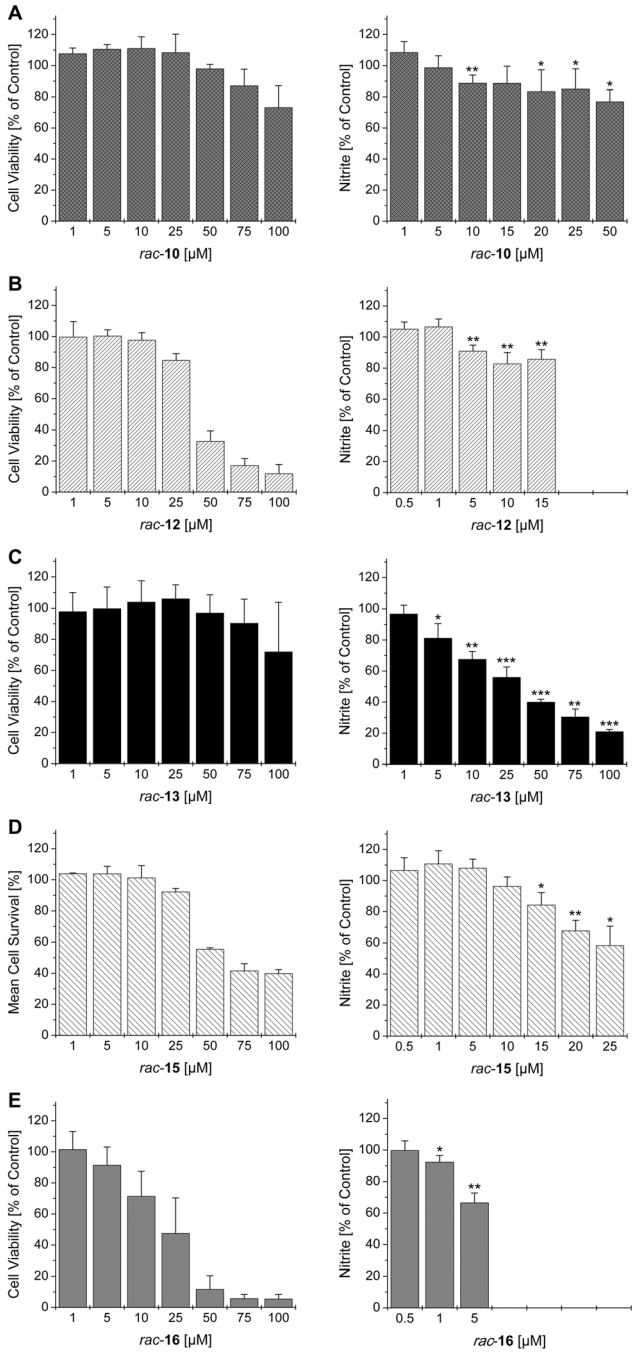

Fig. 6 Results of the *in vitro* assays performed with RAW264.7 cells stimulated with 10 ng mL^{-1} of LPS. Charts on the left side refer to MTT tests (crystal violet assay in the case of *rac*-**15** (D)) after an incubation time of 24 h at different concentrations. Charts on the right display the influence of ET-CORMs on NO-production (Griess assay). Data represent at least three independent experiments performed in quadruplicate. Levels of significance: $*p \leq 0.05$, $**p \leq 0.01$, $***p \leq 0.001$.

strong NO-inhibition of 19–79% at concentrations of 5–100 μM for *rac*-**13** (Fig. 6C) and of 18–83% at 5–100 μM for enone **23** (see also the ESI; Fig. S28B†) which are essentially the same. This indicates that the enone strongly contributes to the overall activity of the complex in this case and might even exceed the activity of the released CO.

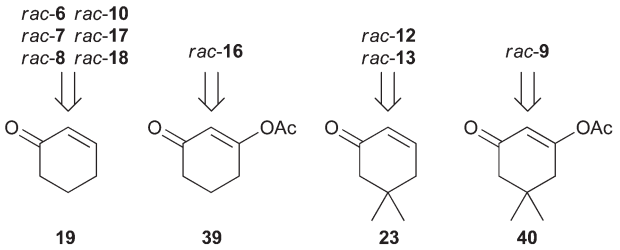

Fig. 7 Structures of tested enones produced from ET-CORMs according to the mechanism shown in Scheme 1.

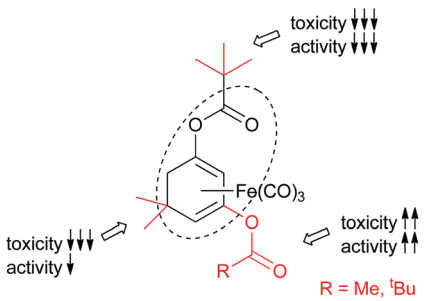

Fig. 8 Influence of modifications of the parent "outer" monoacetate *rac*-**8** (circled substructure) of ET-CORMs on toxicity and activity (inhibition of NO-production). The number of arrows indicates the relative strength of effects.

On cleavage of the "outer" acetate complex *rac*-**8**, *i.e.* the non-dimethylated derivative of *rac*-**13**, enone **19** (cyclohexenone) is liberated, which is a known inducer of phase 2 enzymes through thiol-regulated Michael addition chemistry.[30] Both *rac*-**8** and **19** show equal activity in the Griess assay (10% for *rac*-**8**[14] and 12% NO-inhibition for **19** at 1.0 μM). However, *rac*-**8** exhibits significant toxicity down to 10 μM whereas cyclohexenone displays no toxicity at this concentration (see ESI, Fig. S28A†). This observation points to a distinct CO effect causing the toxicity of *rac*-**8** or a toxic effect of complex *rac*-**8** itself. Furthermore, the comparison of dimethyl-substituted mono-acetoxy-diene complexes *rac*-**11**, *rac*-**12** and *rac*-**13** reveals that in this case the "inner" complexes (*rac*-**11** and *rac*-**12**) are inferior because of their much higher toxicity compared to *rac*-**13**. The inner mono-pivaloate complex *rac*-**7**,[14] the dimethyl-dipivaloate *rac*-**14**, as well as both palmitates (*rac*-**17** and *rac*-**18**) proved to be completely unable to inhibit the production of NO, which indicates poor or no decomposition of these complexes by the intracellular esterases of the particular cell line.

From our biological data we can deduce the structure–activity relationships summarized in Fig. 8. Most importantly, an "outer" dienyl-acetate core-structure (corresponding to *rac*-**8**) proved to be essential for high (desired) biological activity. Introduction of more bulky ester units resulted in reduced NO-inhibition activity together with lower toxicity. The diesters were generally more toxic and exhibited greater NO-inhibition power as compared to the monoesters. Geminal dimethylation at the cyclohexadiene ring reduced the toxicity without inducing a too strong loss of activity. Therefore, *rac*-**9** and *rac*-**13** are the "best" compounds, with *rac*-**9** being more potent but also more toxic than *rac*-**13**.

Overall, *rac*-**13** is considered superior to *rac*-**9** due to its substantially lower cytotoxicity.

Since the (enzyme-triggered) decomposition of the ET-CORMs not only leads to a release of CO (and the enone ligand) but also to the liberation of iron ions, the influence of Fe^{2+} and Fe^{3+} upon the viability and NO-production of RAW264.7 cells was also assessed. Both $FeCl_2$ and $FeCl_3$ proved to be cytotoxic with IC_{20} values (viability) of 34 μM for $FeCl_2$ and 40 μM for $FeCl_3$ together with IC_{50} values >100 μM for both compounds (see ESI†). In contrast to other reports,[28] no influence on the NO-production by Fe^{2+} and Fe^{3+} was observed in the non-toxic concentration range (1 – 25 μM).

Conclusions

We have investigated a series of thirteen acyloxycyclohexadiene–$Fe(CO)_3$ complexes as a powerful new class of CO-releasing molecules (ET-CORMs), which are activated by enzymatic cleavage of the ester functionality. In the course of the study, new efficient synthetic protocols were developed based on the use of (stable) triisopropylsilyloxydiene complexes as intermediates which can be converted into the corresponding esters in a one-step procedure. The complexes prepared (in racemic form) were fully characterized and their ability to release CO upon enzymatic cleavage was investigated in detail. The experimental results (including the consumption of oxygen) are in accordance with the proposed CO release mechanism. In biological investigations the cytotoxicity and the inhibition of NO-production (as an expected consequence of an interaction of CO with iNOS) was assessed using murine macrophage (RAW264.7) cells. In the context of the study, clear structure–activity relationships could be identified. Two ET-CORMs (*rac*-**9** and *rac*-**13**) exhibited particularly promising properties, which to the best of our knowledge make them the most potent CORMs ever studied in this type of assay. We also assessed the biological activity of the expected by-products of the CO release to test whether the biological activity is solely an effect of CO or a combined effect of all the "decomposition" products. These experiments revealed that the enone by-products strongly contribute to the NO-inhibition in the case of the monoesters, but not in the case of the diesters. The iron ions did not induce significant inhibition of the NO-production in the concentrations tested. The results presented here suggest that the iron-based ET-CORMs open up promising options for the future development of small molecules, allowing a controlled and possibly even tissue-selective CO delivery. A next goal is to fine-tune the pharmacological and biological properties, for instance by preparing compounds with higher water solubility.

Experimental

A detailed description of the synthesis of all compounds, including the not commercially available starting materials, of all performed CO-detection experiments (including the measured data) and of the used analytic methods can be found in the ESI.†

NMR spectra were recorded on Bruker instruments (Avance DPX 300, Avance DRX 500 or Avance II 600). UV/Vis spectra were recorded on a Beckmann Coulter DU 800 (cell length 1 cm). IR spectra were recorded on a Perkin-Elmer Paragon 1000 FT-IR spectrometer in the ATR mode at room temperature. Mass spectra were recorded at the Central Analytics Department – Mass Spectroscopy, University of Regensburg and the Analytical Service Unit, University of Cologne on Finnigan instruments (a MAT Inocs 50 galaxy system (for EI LR-MS) and a MAT 900 (for HR-MS)). An Agilent Technologies Model GC 6890N gas chromatograph coupled with an HP 5973N series mass selective detector and an HP 7683 GC autosampler was employed for all GC-MS analyses.

Enantiomeric analyses through GC were performed on an Agilent (HP 6890) instrument with FID detection using either a BGB-176SE column (A) or a 6TBDMS-2,3-Me-β-CD column (B). Enantiomeric analyses through high performance liquid chromatography (HPLC) were conducted with HPLC units from Merck-Hitachi and Knauer (UV-detection at 220 nm and 254 nm) using one of the following columns: Diacel Chiracel OD-H (1), Diacel Chiracel OJ (2), Diacel Chiralpak AD-H (3), Macherey Nagel Nucleocell (4) and *n*-Hex–*i*-PrOH (99 : 1, 98 : 2 or 95 : 5) as a solvent. Gas chromatograms for the CO-detection were recorded using a Varian CP-3800 gas chromatograph with helium as the carrier gas and a 3 m × 2 mm packed molecular sieve 13× 80–100 column. The gases were detected using a thermal conductivity detector (Varian) operated at 150 °C. CHN analyses were conducted on an Elementar Vario EL machine.

All reactions were carried out in flame-dried glassware under an argon atmosphere. Chemicals were purchased from Merck, Sigma-Aldrich, Fluka, Acros, Lancaster or Strem and used without further purification. Solvents were dried following standard procedures (ESI†). The release of CO *via* the Mb-assay was performed as previously described.[14]

Crystallographic details

Measurements were made on a Nonius Kappa-CCD diffractometer with Mo-Kα radiation (λ = 0.71073), and Denzo was used for data reduction. The structures were solved by direct methods (Shelxs97).[33] Shelxl97 was used for full-matrix least-squares refinement on F^2. All non-hydrogen atoms were refined anisotropically. All hydrogen atoms were placed in geometrically idealized positions and refined by using a riding model. Ortep plots were generated with Platon.[34] The absorption correction (X-RED) was performed after optimizing the crystal shape using X-SHAPE. Crystal structure determination details are summarized in Table 4.

Detection of the CO release by GC

All reactions were performed in headspace vials – 10 mL (BGB-analytics, Cat. No. 200410-F). Prior to the detection of the CO release, a calibration was done using the same solvent mixture (1 mL of phosphate buffer (0.1 M, pH = 7.4) and 0.2 mL of DMSO) that was used for the CO release experiments. For the CO calibration, the consumption of oxygen had to be included. For this purpose the reaction vial was filled with the solvent mixture and completely degassed with nitrogen. Afterwards, 21% of the gas volume was replaced by oxygen to generate the composition of air (2.250 mL). To generate gas mixtures that are

Table 4 Crystal data, data collection and refinement parameters for *rac*-**10**, *rac*-**11**, *rac*-**12**, *rac*-**14**, *rac*-**15**, *rac*-**17** and *rac*-**18**

	rac-**10**	*rac*-**11**	*rac*-**12**	*rac*-**14**	*rac*-**15**	*rac*-**17**	*rac*-**18**
Empirical formula	$C_{14}H_{16}FeO_5$	$C_{13}H_{14}FeO_5$	$C_{13}H_{14}FeO_5$	$C_{21}H_{28}FeO_7$	$C_{19}H_{24}FeO_7$	$C_{25}H_{38}FeO_5$	$C_{25}H_{38}FeO_5$
M (g mol^{-1})	320.12	306.09	306.09	448.28	420.23	474.40	474.40
Crystal system	Monoclinic	Monoclinic	Triclinic	Triclinic	Monoclinic	Triclinic	Triclinic
Space group	$P2_1/c$	$P2_1/c$	$P\bar{1}$	$P\bar{1}$	$P2_1/c$	$P\bar{1}$	$P\bar{1}$
a (Å)	12.4124(4)	9.6264(7)	6.1260(4)	11.0195(8)	13.5179(16)	8.6905(3)	6.6635(14)
b (Å)	6.4417(2)	14.1259(7)	7.5018(5)	13.4293(8)	12.1754(7)	10.0025(4)	6.7003(15)
c (Å)	18.6015(7)	11.9873(7)	15.0179(10)	16.2464(10)	12.5175(15)	28.6690(12)	28.213(6)
α (°)	90	90	77.693(4)	75.189(4)	90	89.975(2)	85.849(5)
β (°)	104.644(2)	124.757(4)	89.267(3)	86.972(3)	100.201(3)	87.653(2)	86.939(6)
γ (°)	90	90	78.463(3)	89.571(3)	90	82.287(2)	82.030(7)
V (Å^3)	1439.00(8)	1339.21(16)	660.36(8)	2321.0(3)	2027.6(4)	2467.45(17)	1243.0(5)
T (K)	100(2)	100(2)	100(2)	150(2)	100(2)	100(2)	100(2)
Z	4	4	2	4	4	4	2
D_c (g cm^{-3})	1.478	1.518	1.539	1.283	1.377	1.277	1.268
Crystal size (mm^3)	0.2 × 0.15 × 0.07	0.2 × 0.07 × 0.02	0.2 × 0.2 × 0.07	0.2 × 0.2 × 0.1	0.1 × 0.07 × 0.02	0.15 × 0.05 × 0.01	0.3 × 0.1 × 0.03
θ range (°)	1.70 to 26.99	2.52 to 26.99	1.39 to 26.99	1.30 to 27.00	1.53 to 25.00	1.42 to 27.00	1.45 to 25.00
No. data collected	13 203	6848	4112	15 189	12 099	16 558	5290
No. unique data	3140	2918	2877	10 119	3374	10 724	4158
Final R indices [$I > 2\sigma(I)$]	R_1 = 0.0285, wR_2 = 0.0734	R_1 = 0.0322, wR_2 = 0.0734	R_1 = 0.0233, wR_2 = 0.0572	R_1 = 0.0667, wR_2 = 0.1514	R_1 = 0.0606, wR_2 = 0.1592	R_1 = 0.0579, wR_2 = 0.1363	R_1 = 0.0745, wR_2 = 0.1718
R indices (all data)	R_1 = 0.0358, wR_2 = 0.0756	R_1 = 0.0540, wR_2 = 0.0800	R_1 = 0.0277, wR_2 = 0.0627	R_1 = 0.1565, wR_2 = 0.1848	R_1 = 0.0916, wR_2 = 0.1803	R_1 = 0.0986, wR_2 = 0.1561	R_1 = 0.1435, wR_2 = 0.2007
Largest diff. peak/hole (e Å^{-3})	0.452/−0.374	0.533/−0.466	0.360/−0.261	0.560/−0.420	1.017/−0.510	1.027/−0.670	1.091/−0.413

formed when a particular amount of O_2 is consumed in the course of the CO release, the volume of added oxygen was decreased by the amount that is theoretically needed for the release of the added CO. The resulting gas mixture was warmed to 37 °C for 10 min prior to the injection and analysis of 50 µL samples by GC. The determined areas from the GC signals were plotted against the amount of O_2 or CO (calculated with the ideal gas law) and fitted (linear for 1.0 equiv., 1.5 equiv. and 2.0 equiv. and exponential for 4.0 equiv. and no O_2 consumption). Thus, for the CO and O_2 calibration, different equivalents of released CO per consumed O_2 were used (1.0 equiv., 1.5 equiv., 2.0 equiv., 4.0 equiv. and no O_2 consumption) and the calibration data were compared to the experimental data of the CO release curves. The data for 1.0 equiv., 1.5 equiv. and 2.0 equiv. matched best and were quite similar. Therefore, an average of the three slopes was taken for the calculation of the released CO.

To monitor the enzyme-triggered CO release, the particular complex (36 µmol) was dissolved in DMSO (0.2 mL) and phosphate buffer (1 mL; 0.1 M, pH = 7.4) was added. The particular enzyme (15 mg of PLE or 20 mg of LCR) was added and the vial was closed with a rubber vial cap. The reaction mixture was stirred at 37 °C. From time to time samples (50 µL) were taken and the CO release was quantified. The half-life times were determined directly from an exponential fit of the CO-release (first or second order).

Cells and cell culture

The murine macrophage cell line RAW264.7[35] was kept under standard cell culture conditions using RPMI with 10% heat-inactivated fetal calf serum (FCS) and 2 mM glutamine (Invitrogen, Karlsruhe, Germany).

Determination of cell viability by MTT assay

Cell viability was evaluated by MTT assay as described before.[14] In brief, cells were seeded in 96-well plates at a density of 5 × 10^3 per well, cultured for 24 h, and then incubated for another 24 h with medium supplemented with compounds and 10 ng mL^{-1} of LPS (Sigma). Controls received only culture medium with LPS or with solvent and LPS. Afterwards, supernatants were removed, 100 µL of MTT solution was added to each well, and cells were incubated for another 3 h at 37 °C. Subsequently, 100 µL of SDS-solution (10%) was added, and formazan was allowed to dissolve overnight. Absorbance was determined at 560 nm with a multi-well plate photometer (TiterTek).

Determination of cell proliferation by crystal violet staining

The crystal violet staining was used if it was not possible to get a reliable result in the MTT test because of interference of the substances with MTT, and was performed as described previously.[14] In brief, cells were seeded in 96-well plates at a density of 5 × 10^3 per well, cultured for 24 h, and then treated according to the MTT assay. Afterwards, supernatants were removed and cells were stained with 30 µL crystal violet solution per well for 10 min. Crystal violet was removed, cells were washed with 200 µL aqua dest. and allowed to air-dry overnight. Crystal violet was then solubilized by addition of 100 µL EtOH–

Na-citrate solution per well and absorbance was determined at 560 nm.

Measurement of nitrite production by Griess assay

Generation of NO was determined by the Griess reaction which is based on the detection of accumulating nitrite in the cell culture medium.[36] The assay was performed as described previously.[14] Briefly, cells were seeded in 96-well plates at a density of 8×10^4 per well, cultured for 24 h and subsequently incubated for another 24 h with medium supplemented with compounds and 10 ng mL^{-1} of LPS. Afterwards a volume of 100 µL culture supernatant was mixed with 100 µL of Griess reagent. After 15 min incubation at room temperature, absorbance was determined at 560 nm. The nitrite content was determined by using sodium nitrite as the standard.

Data evaluation/statistical analysis

Experiments were carried out with at least four parallels and repeated independently at least three times. Results are expressed as mean ± SD and are depicted as a percentage of untreated controls. A sigmoidal logistic function was used to fit dose–response curves and to determine IC_{50} and IC_{20} values, using a Microsoft Excel calculation sheet (Ed50plus, v1.0, April 2000, Mario H. Vargas, Instituto Nacional de Enfermedades, Mexico). Statistical analysis was performed using the software Prism (GraphPad Software). Quantitative data were tested with a two-tailed paired Student's *t*-test referring to the untreated control. Levels of significance: $*p \leq 0.05$, $**p \leq 0.01$, $***p \leq 0.001$.

Syntheses

Synthesis of the γ-pivalate substituted enones 28 and 29. A solution of cyclohexa-1,3-dione (1.0 equiv.) and pyridine (2.0 equiv.) in DCM was cooled to 0 °C. Pivaloyl chloride (1.5 equiv.) was added dropwise and the reaction mixture was stirred (1 h). Afterwards water was added, the phases were separated and the aqueous phase was extracted with DCM. The combined organic phases were dried over anhydrous $MgSO_4$, the solvent was evaporated and the raw product was purified by column chromatography.

3-Oxocyclohex-1-en-1-yl pivalate (28). Yield: 11.5 g (29.2 mmol, 82%). FT-IR (ATR): ν [cm^{-1}] = 2971 (m, C_{sp3}–H), 2874 (m, C_{sp3}–H), 1748 (s, C═O). ^{1}H NMR (300 MHz, $CDCl_3$): δ = 5.80 (s, 1H, H2), 2.46 (t, J = 6.1 Hz, 2H, H4), 2.35 (t, J = 6.7 Hz, 2H, H6), 2.08–1.93 (Ψq, J = 6.4 Hz, 2H, H5), 1.22 (s, 9H, H9). ^{13}C NMR (75 MHz, $CDCl_3$): δ = 199.4 (C3), 175.1 (C7), 170.3 (C1), 117.4 (C2), 39.2 (C8), 36.6 (C4), 28.1 (C6), 26.8 (C9), 21.2 (C5). LR-MS (GC-MS): m/z (%) = 196 (1, $[M]^+$), 153 (3), 125 (4), 113 (35), 96 (4), 85 (71), 83 (43), 69 (21), 57 (100).

5,5-Dimethyl-3-oxocyclohex-1-en-1-yl pivalate (29). Yield: 14.37 g (68.04 mmol, 90%). mp < 30 °C (from DCM). FT-IR (ATR): ν [cm^{-1}] = 2966 (w, C_{sp3}–H), 2866 (w, C_{sp3}–H), 1754 (m, C═O). ^{1}H NMR (300 MHz, $CDCl_3$): δ = 5.86 (s, 1H, H2), 2.40 (s, 2H, H4), 2.27 (s, 2H, H6), 1.28 (s, 9H, H11), 1.12 (s, 6H, H7, H8). ^{13}C NMR (75 MHz, $CDCl_3$): δ = 199.3 (C3), 175.4 (C9), 168.7 (C1), 116.6 (C2), 50.8 (C4), 42.0 (C6), 39.3 (C10), 33.1 (C5), 28.2 (C11), 26.9 (C7, C8). GC-MS: m/z (%) = 224 (<1, $[M]^+$), 181 (4), 141 (66, $[M - C_5H_7O]^+$), 112 (10), 85 (100), 57 (100), 41 (50).

General procedure 1 for dienyl-ester and silyldienol ether formation

To a solution of diisopropylamine (*ca.* 1.5 equiv.) in THF was added *n*-butyllithium (*ca.* 1.3 equiv.) at −78 °C. After stirring the mixture for 10 min, a solution of the particular enone (1 equiv.) in THF was added dropwise (*ca.* 1 h). Stirring was continued for 1 h at −78 °C. Afterwards the particular electrophile (2.5 equiv., 1.2 equiv. for TIPSOTf) in THF was added dropwise (1 h). After 30 min at −78 °C the reaction mixture was allowed to warm to 25 °C before it was quenched by addition of saturated aqueous NH_4Cl. After 10 min the mixture was extracted with M*t*BE and the organic layer was washed with water and brine and dried over anhydrous $MgSO_4$. Finally, the solvent was evaporated and the crude product was purified by column chromatography.

4,4-Dimethylcyclohexa-1,5-dien-1-yl acetate (22). Yield: 1.49 g (8.8 mmol, 70%). FT-IR (ATR): ν [cm^{-1}] = 3017 (w, C_{sp2}–H), 2957 (s, C_{sp3}–H), 2866 (m, C_{sp3}–H), 2819 (w, C_{sp3}–H), 1759 (s, C═O). ^{1}H NMR (300 MHz, $CDCl_3$): δ = 5.55 (m, 2H, H6, H5), 5.24 (m, 1H, H2), 2.19 (d, J = 1.0 Hz, 2H, H3), 2.09 (s, 3H, H9), 1.01 (s, 6H, H7). ^{13}C NMR (75 MHz, $CDCl_3$): δ = 169.2 (C8), 145.0 (C1), 140.0 (C5), 120.4 (C6), 109.8 (C2), 36.5 (C3), 31.2 (C4), 27.6 (C7), 20.9 (C9). LR-MS (GC-MS): m/z (%) = 166 (20, $[M]^+$), 124 (46), 109 (100), 91 (15), 81 (15), 67 (8), 55 (10), 43 (14).

3,3-Dimethylcyclohexa-1,5-dien-1-yl acetate (24). Yield: 1.361 g (8.1 mmol, 65%). FT-IR (ATR): ν [cm^{-1}] = 2955 (m, C_{sp3}–H), 2923 (m, C_{sp3}–H), 2865 (w, C_{sp3}–H), 1759 (s, C═O). ^{1}H NMR (300 MHz, $CDCl_3$): δ = 5.83–5.74 (m, 1H, H6), 5.66 (ddd, J = 9.9, 3.7, 1.9 Hz, 1H, H5), 5.10 (Ψd, J = 1.7 Hz, 1H, H2), 2.12 (Ψdd, J = 4.3, 1.9 Hz, 2H, H4), 2.10 (s, 3H, H8), 1.02 (s, 6H, H9, H10). ^{13}C NMR (75 MHz, $CDCl_3$): δ = 169.2 (C7), 144.4 (C1), 127.7 (C6), 122.0 (C5), 121.9 (C2), 37.5 (C4), 31.7 (C3), 28.1 (C9, C10), 21.0 (C8). LR-MS (GC-MS): m/z (%) = 166 (9, $[M]^+$), 124 (10, $[M - (CH_2CO)]^+$), 109 (100), 91 (9), 79 (10), 68 (8), 43 (20).

Cyclohexa-1,3-diene-1,3-diyl dipivalate (30). Yield: raw product containing *ca.* 583 mg (2.08 mmol, 40%). FT-IR (ATR): ν [cm^{-1}] = 2971 (m, C_{sp3}–H), 2880 (w, C_{sp3}–H), 1747 (s, C═O). ^{1}H NMR (300 MHz, $CDCl_3$): δ = 5.50 (s, 1H, H2), 5.26 (s, 1H, H4), 2.59–2.23 (m, 4H, H5, H6), 1.25 (s, 18H, H9, H12). ^{13}C NMR (75 MHz, $CDCl_3$): δ = 176.9 (C7/C10), 176.3 (C7/C10), 151.0 (C1/C3), 144.9 (C1/C3), 110.0 (C2), 107.7 (C4), 39.0 (C8/C11), 38.8 (C8/C11), 27.0 (C9, C12), 25.3 (C6), 21.6 (C5). LR-MS (GC-MS): m/z (%) = 280 (4, $[M]^+$), 196 (10), 112 (39), 85 (10), 68 (25), 57 (100), 41 (61).

5,5-Dimethylcyclohexa-1,3-diene-1,3-diyl dipivalate (31). Yield: 1.77 g (5.8 mmol, 46%). mp < 30 °C (from DCM). FT-IR (ATR): ν [cm^{-1}] = 2965 (m, C_{sp3}–H), 2866 (w, C_{sp3}–H),

1747 (s, C═O). ^{1}H NMR (300 MHz, $CDCl_3$): δ = 5.49 (s, 1H, H2), 5.06 (Ψd, J = 1.2 Hz, 1H, H6), 2.28 (s, 2H, H4), 1.25 (s, 18H, H11, H14), 1.14 (s, 6H, H7, H8). ^{13}C NMR (75 MHz, $CDCl_3$): δ = 176.9 (C9/C12), 176.6 (C9/C12), 150.4 (C1/C3), 143.2 (C1/C3), 119.1 (C2), 109.1 (C6), 40.3 (C4), 39.0 (C10/C13), 38.8 (C10/C13), 33.2 (C5), 28.3 (C7, C8), 27.0 (C11, C14). GC-MS: m/z (%) = 308 (8, $[M]^+$), 224 (11, $[M - C_5H_8O]^+$), 209 (25), 140 (7), 125 (41), 109 (4), 85 (8), 57 (100), 41 (36).

(Cyclohexa-1,5-dien-1-yloxy)triisopropylsilane (33). Yield: 3.77 g (15.5 mmol, 99%). FT-IR (ATR): ν [cm^{-1}] = 3020 (w, C_{sp2}–H), 2940 (s, C_{sp3}–H), 2860 (s, C_{sp3}–H), 1700 (m), 1646 (s). ^{1}H NMR (300 MHz, $CDCl_3$): δ = 5.87–5.83 (m, 1H, H5), 5.76–5.72 (d, J = 6.0 Hz, 1H, H6), 4.89 (Ψs, 1H, H2), 2.14–2.07 (m, 4H, H3, H4), 1.17–1.10 (d, J = 1.1 Hz, 18H, H8), 1.07–1.05 (m, 3H, H7). ^{13}C NMR (75 MHz, $CDCl_3$): δ = 148.6 (C1), 128.7 (C5), 126.7 (C6), 101.9 (C2), 22.6–21.8 (C3/C4), 17.9 (C8), 12.5 (C7). LR-MS (GC-MS): m/z (%) = 252 (100, $[M]^+$), 237 (1), 209 (30), 179 (50), 151 (83), 121 (16), 103 (11), 75 (36), 59 (35), 41 (28). HR-MS (DIP-MS, 70 eV): m/z 252.191 (calcd ($[M]^+$) m/z 252.1909).

General procedure 2 for dienyl-ester and silyldienol ether formation

To a solution of hexamethyldisilazane (1.5 equiv.) in THF was added *n*-butyllithium (1.3 equiv.) at −78 °C. After 10 min TPPA (2.5 equiv.) was added and stirring was continued for 20 min at −78 °C. Then the particular enone (1.0 equiv.) in THF was added dropwise (1 h). Afterwards the particular electrophile (2.5 equiv., 1.2 equiv. for TIPSOTf) in THF was added dropwise (1 h). The mixture was stirred for an additional 30 min at −78 °C and then allowed to warm to 25 °C before it was quenched with saturated aqueous NH_4Cl. After extraction with M*t*BE, the organic solution was washed with water and brine and dried over anhydrous $MgSO_4$. Finally, the solvent was evaporated and the crude product was purified by column chromatography.

Cyclohexa-1,3-dienyl pivalate (20). Yield: 900 mg (5.0 mmol, 62%). FT-IR (ATR): ν [cm^{-1}] = 2968 (w, C_{sp3}–H), 2933 (s, C_{sp3}–H), 2871 (m, C_{sp3}–H), 1741 (s, C═O). ^{1}H NMR (500 MHz, $CDCl_3$): δ = 5.94–5.77 (m, 1H, H3), 5.70–5.51 (m, 2H, H2, H4), 2.43–2.21 (m, 4H, H5, H6), 1.23 (s, 9H, H9). ^{13}C NMR (125 MHz, $CDCl_3$): δ = 176.7 (C7), 149.4 (C1), 123.3 (C3/C4), 122.9 (C3/C4), 110.6 (C2), 38.9 (C8), 27.0 (C9), 25.3 (C5/C6), 23.6 (C5/C6). LR-MS (GC-MS): m/z (%) = 180 (10, $[M]^+$), 96 (98), 79 (12), 67 (15), 57 (100, $[C(CH_3)_3]^+$), 41 (47).

(Cyclohexa-1,3-dien-1-yloxy)triisopropylsilane (37). Yield: 1.90 g (7.5 mmol, 85%). FT-IR (ATR): ν [cm^{-1}] = 3039 (w, C_{sp2}–H), 2941 (s, C_{sp3}–H), 2889 (m, C_{sp3}–H), 2864 (s, C_{sp3}–H). ^{1}H NMR (300 MHz, $CDCl_3$): δ = 5.94–5.69 (m, 1H, H3), 5.39 (Ψdd, J = 9.2, 3.8 Hz, 1H, H4), 5.12 (d, J = 5.8 Hz, 1H, H2), 2.25 (Ψd, J = 12.0 Hz, 4H, H5, H6), 1.24–1.15 (m, 3H, H7), 1.10 (s, 12H, H8), 1.08 (s, 6H, H8). ^{13}C NMR (75 MHz, $CDCl_3$): δ = 154.1 (C1), 124.7 (C3), 117.8 (C4), 101.7 (C2), 28.7 (C5/C6), 24.0 (C5/C6), 17.9 (C7), 12.6 (C8). LR-MS (GC-MS): m/z (%) = 252 (90, $[M]^+$), 207 (59), 179 (59), 151 (100), 137 (71), 121 (23), 77 (37), 59 (26), 41 (23).

5,5-Dimethylcyclohexa-1,3-dien-1-yl acetate (25). Yield: 881 mg (5.3 mmol, 65%). FT-IR (ATR): ν [cm^{-1}] = 2946 (m, C_{sp3}–H), 2920 (s, C_{sp3}–H), 2851 (m, C_{sp3}–H), 1756 (s, C═O). ^{1}H NMR (300 MHz, $CDCl_3$): δ = 5.70 (dd, J = 9.4, 5.8 Hz, 1H, H3), 5.57 (d, J = 5.8 Hz, 1H, H4), 5.37 (d, J = 9.4 Hz, 1H, H2), 2.22 (Ψd, J = 1.1 Hz, 2H, H6), 2.11 (s, 3H, H8), 1.04 (s, 6H, H9, H10). ^{13}C NMR (75 MHz, $CDCl_3$): δ = 169.0 (C7), 148.7 (C1), 135.2 (C2), 119.8 (C3), 109.6 (C4), 40.3 (C6), 33.8 (C5), 27.9 (C9, C10), 21.0 (C8). LR-MS (GC-MS): m/z (%) = 166 (17, $[M]^+$), 124 (26, $[M - (CH_2CO)]^+$), 109 (100), 91 (9), 79 (10), 43 (25).

General preparation of diene–$Fe(CO)_3$ complexes

A Schlenk tube was charged with the diene (1 equiv.) and $Fe_2(CO)_9$ (2–3 equiv.) and set under argon by three evacuation/argon flush cycles. Then, degassed diethyl ether was added and the reaction mixture was heated to reflux for 20 h under argon. Finally, the solvent was evaporated and the crude mixture was purified by column chromatography to yield the desired complex.

(*RS*)-Tricarbonyl-η^4-(1-hexadecanoyloxy-1,5-cyclohexadiene)-iron(0) (*rac*-17). Without column chromatography, the solvent was evaporated, the residue was dissolved in DMF and the solution was added to NaH (3.7 equiv.). The reaction mixture was cooled (0 °C) and TBAF (1.8 equiv.) was added dropwise. After 45 min palmitoyl chloride (2.0 equiv.) was added and the reaction was stirred at 20 °C (3 h, TLC). After workup and purification by column chromatography (DCM–CyHex = 1 : 3), 986 mg (2.08 mmol, 62%) of complex *rac*-**17** were isolated as a yellow solid. mp 36.7 °C (DCM). EA: Calcd for $C_{25}H_{38}FeO_5$: C 63.29; H 8.07. Found: C 62.81; H 8.15. FT-IR (ATR): ν [cm^{-1}] = 2921 (s, C_{sp3}–H), 2851 (m, C_{sp3}–H), 2045 (s, $Fe(CO)_3$), 1967 (bs, $Fe(CO)_3$), 1762 (m, C═O). ^{1}H NMR (500 MHz, $CDCl_3$): δ = 5.53 (Ψdd, J = 6.6, 1.2 Hz, 1H, H6), 3.38 (Ψdt, J = 3.8, 2.2 Hz, 1H, H2), 2.88 (dt, J = 6.4, 2.9 Hz, 1H, H5), 2.45 (t, J = 7.5 Hz, 2H, H8), 1.91–1.74 (m, 2H, H3), 1.73–1.65 (m, 2H, H21), 1.62–1.54 (m, 2H, H4), 1.41–1.25 (m, 24H, H9–H20), 0.90 (t, J = 7.0 Hz, 3H, H22). ^{13}C NMR (126 MHz, $CDCl_3$): δ = 210.5 ($Fe(CO)_3$), 173.0 (C7), 128.1 (C1), 79.4 (C6), 58.9 (C2), 51.7 (C5), 33.9 (C8), 31.7 (C9–C20), 29.4 (C9–C20), 29.4 (C9–C20), 29.4 (C9–C20), 29.3 (C9–C20), 29.2 (C9–C20), 29.1 (C9–C20), 28.9 (C9–C20), 28.7 (C9–C20), 24.7 (C3/C21), 24.5 (C3/C21), 23.2 (C4), 22.4 (C9–C20), 13.9 (C22). LR-MS (DIP-MS, 70 eV): m/z (%) = 446 (1, $[M - CO]^+$), 418 (5, $[M - 2CO]^+$), 390 (100, $[M - 3CO]^+$), 310 (29), 309 (35), 226 (34), 212 (56), 198 (39), 184 (25), 170 (19), 156 (17), 151 (40), 97 (36), 83 (28), 71 (37), 57 (87), 56 (46, $[Fe]^+$). HR-MS (DIP-MS, 70 eV): m/z 418.217 ± 0.0021 (calcd ($[M - 2CO]^+$): m/z 418.2170).

(*RS*)-Tricarbonyl-η^4-(1-triisopropylsiloxy-1,3-cyclohexadiene)-iron(0) (*rac*-38). Yield: 1.38 g (3.51 mmol, 89%). FT-IR (ATR): ν [cm^{-1}] = 2942 (s, C_{sp3}–H), 2889 (m, C_{sp3}–H), 2865 (s, C_{sp3}–H), 2031 (s, $Fe(CO)_3$), 1948 (bs, $Fe(CO)_3$). ^{1}H NMR (300 MHz, $CDCl_3$): δ = 5.18 (d, J = 4.3 Hz, 1H, H2), 5.94 (Ψt, J = 9.0 Hz,

1H, H3), 2.89–2.78 (m, 1H, H4), 2.28–2.10 (m, 1H, H6), 2.06–1.81 (m, 2H, H5, H6), 1.68–1.75 (m, 1H, H5), 1.09 (s, 21H, H7, H8). ^{13}C NMR (75 MHz, $CDCl_3$): δ 213.3 ($Fe(CO)_3$), 113.9 (C1), 78.1 (C2), 76.0 (C3), 56.7 (C4), 31.0 (C6), 24.6 (C5), 18.0 (C8), 13.2 (C7). LR-MS (DIP-MS, 70 eV): *m/z* (%) = 392 (1, $[M]^+$), 364 (32, $[M - CO]^+$), 336 (9, $[M - 2CO]^+$), 334 (25), 308 (7, $[M - 3CO]^+$), 306 (95), 290 (15), 265 (17), 264 (100), 252 (16), 248 (21), 222 (33), 207 (15), 179 (15), 164 (11), 151 (20), 137 (17), 121 (5), 100 (5). HR-MS (DIP-MS, 70 eV): *m/z* 364.116 (calcd ($[M - CO]^+$): *m/z* 364.1157).

(*RS*)-Tricarbonyl-η^4-(1-triisopropylsiloxy-1,5-cyclohexadiene)-iron(0) (*rac*-35). Yield: 2.85 g (7.28 mmol, 92%). FT-IR (ATR): ν [cm^{-1}] = 2944 (s, C_{sp3}–H), 2889 (m, C_{sp3}–H), 2865 (s, C_{sp3}–H), 2040 (s, $Fe(CO)_3$), 1960 (bs, $Fe(CO)_3$). ^{1}H NMR (300 MHz, $CDCl_3$): δ = 5.28 (d, *J* = 6.5 Hz, 1H, H6), 3.39 (Ψs, 1H, H2), 2.70 (d, *J* = 2.7 Hz, 1H, H6), 1.84–1.62 (m, 2H, H3), 1.48 (Ψddd, *J* = 19.3, 14.4, 9.0 Hz, 2H, H4), 1.22 (Ψdd, *J* = 14.4, 6.9 Hz, 3H, H7), 1.11 (s, 18H, H8). ^{13}C NMR (75 MHz, $CDCl_3$): δ = 211.6 ($Fe(CO)_3$), 136.5 (C1), 76.7 (C6), 58.6 (C2), 50.5 (C5), 25.4 (C3), 23.1 (C4), 17.7 (C8), 12.4 (C7). LR-MS (DIP-MS, 70 eV): *m/z* (%) = 392 (2, $[M]^+$), 364 (31, $[M - CO]^+$), 336 (9, $[M - 2CO]^+$), 334 (30), 308 (14, $[M - 3CO]^+$), 306 (100), 290 (30), 265 (17), 264 (98), 252 (5), 248 (19), 222 (45), 207 (15), 179 (15), 164 (25), 151 (10), 137 (15), 121 (9), 100 (5). HR-MS (DIP-MS, 70 eV): *m/z* 364.115 ± 0.0004 (calcd ($[M - CO]^+$): *m/z* 364.1157).

(*RS*)-Tricarbonyl-η^4-(1-hexadecanoyloxy-1,3-cyclohexadiene)-iron(0) (*rac*-18). A solution of TBAF (2.5 mL, 3.00 mmol, 1.2 M in THF, 3.5 equiv.) was added to a solution of complex *rac*-**38** (333 mg, 0.85 mmol, 1 equiv.) in DMF (10 mL) and the mixture was stirred (10 min, TLC). Afterwards DIPEA (0.51 mL, 3.0 mmol, 3.5 equiv.) was added, followed by the addition of palmitoyl chloride (0.91 mL, 3.0 mmol, 3.5 equiv.). After stirring at 20 °C to completion (10 min, TLC), the reaction was quenched by the addition of water and extracted with hexane and M*t*BE. The combined organic solvents were dried over $MgSO_4$ and evaporated. After purification by column chromatography (DCM–CyHex = 1 : 3), 393 mg (0.83 mmol, 97%) of complex *rac*-**18** were isolated as a yellow solid. mp 29.5 °C (from DCM). EA: Calcd for $C_{25}H_{38}FeO_5$: C 63.29; H 8.07. Found: C 63.45; H 8.08. FT-IR (ATR): ν [cm^{-1}] = 2920 (s, C_{sp3}–H), 2850 (s, C_{sp3}–H), 2046 (s, $Fe(CO)_3$), 1962 (bs, $Fe(CO)_3$), 1748 (s, C═O). ^{1}H NMR (500 MHz, $CDCl_3$): δ = 5.39 (d, *J* = 4.3 Hz, 1H, H2), 5.21–5.06 (m, 1H, H3), 3.11 (ddd, *J* = 5.5, 3.8, 1.8 Hz, 1H, H4), 2.32 (t, *J* = 7.6 Hz, 2H, H8), 2.17 (ddd, *J* = 12.6, 3.0, 1.6 Hz, 1H, H6), 1.89 (ddt, *J* = 15.0, 11.6, 3.4 Hz, 1H, H5), 1.84–1.75 (m, 1H, H6), 1.75–1.66 (m, 1H, H6), 1.63 (dd, *J* = 14.2, 7.3 Hz, 2H, H21), 1.36–1.23 (m, 24H, H9–H20), 0.90 (t, *J* = 6.9 Hz, 3H, H22). ^{13}C NMR (126 MHz, $CDCl_3$): δ = 211.3 ($Fe(CO)_3$), 172.0 (C7), 103.2 (C1), 80.5 (C3), 80.3 (C2), 60.2 (C4), 34.5 (C8), 31.9 (C9–C20), 29.7 (C9–C20), 29.7 (C9–C20), 29.6 (C9–C20), 29.6 (C9–C20), 29.4 (C9–C20), 29.4 (C9–C20), 29.2 (C9–C20), 29.0 (C9–C20), 26.7 (C6), 24.8 (C21), 24.0 (C5), 22.7 (C9–C20), 14.1 (C22). LR-MS (DIP-MS, 70 eV): *m/z* (%) = 446 (2, $[M - CO]^+$), 418 (6, $[M - 2CO]^+$), 390 (100, $[M - 3CO]^+$), 362 (4), 334 (6), 310 (17), 309 (28), 254 (18), 240 (22), 198 (15), 156 (8), 149 (21), 134 (14), 97 (12), 96 (40), 57 (33), 56 (22, $[Fe]^+$). HR-MS (DIP-MS, 70 eV): *m/z* 446.2115 ± 0.0004 (calcd ($[M - CO]^+$): *m/z* 446.2119).

(*RS*)-Tricarbonyl-η^4-(1-acetoxy-3,3-dimethyl-1,5-cyclohexadiene)-iron(0) (*rac*-12). Yield: 525 mg (1.72 mmol, 57%). mp 54.1 °C (from DCM). EA: Calcd for $C_{13}H_{14}FeO_5$: C 51.01; H 4.61. Found: C 51.00; H 4.65. FT-IR (ATR): ν [cm^{-1}] = 2953 (m, C_{sp3}–H), 2866 (w, C_{sp3}–H), 2043 (s, $Fe(CO)_3$), 1961 (bs, $Fe(CO)_3$), 1767 (s, C═O). ^{1}H NMR (600 MHz, $CDCl_3$): δ = 5.62 (d, *J* = 6.0 Hz, 1H, H6), 3.07 (Ψd, *J* = 2.0 Hz, 1H, H2), 2.75–2.72 (m, 1H, H5), 2.17 (s, 3H, H8), 1.56–1.41 (m, 2H, H4), 1.08 (s, 3H, H9/H10), 1.03 (s, 3H, H9/H10). ^{13}C NMR (150 MHz, $CDCl_3$): δ = 211.0 ($Fe(CO)_3$), 169.7 (C7), 126.6 (C1), 81.1 (C6), 71.1 (C2), 51.4 (C5), 42.1 (C4), 36.1 (C3), 34.6 (C9/C10), 30.8 (C9/C10), 21.2 (C8). LR-MS (DIP-MS, 70 eV): *m/z* (%) = 278 (12, $[M - CO]^+$), 250 (26, $[M - 2CO]^+$), 222 (24, $[M - 3CO]^+$), 206 (100), 178 (12), 164 (19), 146 (9), 134 (10), 109 (17), 97 (24), 91 (14), 71 (8), 68 (12), 56 (57, $[Fe]^+$). HR-MS (DIP-MS, 70 eV): *m/z* 278.0145 ± 0.0004 (calcd ($[M - CO]^+$): *m/z* 278.0241).

(*RS*)-Tricarbonyl-η^4-(1-acetoxy-4,4-dimethyl-1,5-cyclohexadiene)-iron(0) (*rac*-11). Yield: 659 mg (2.15 mmol, 72%). mp 44.7 °C (from DCM). EA: Calcd for $C_{13}H_{14}FeO_5$: C 51.01; H 4.61. Found: C 51.27; H 4.69. FT-IR (ATR): ν [cm^{-1}] = 2995 (m, C_{sp3}–H), 2859 (w, C_{sp3}–H), 2043 (s, ($Fe(CO)_3$), 1967 (bs, $Fe(CO)_3$), 1762 (s, C═O). ^{1}H NMR (500 MHz, $CDCl_3$): δ = 5.45 (Ψdd, *J* = 1.9, 6.6 Hz, 1H, H6), 3.20 (dd, *J* = 2.7, 4.9 Hz, 1H, H2), 2.50 (d, *J* = 6.3 Hz, 1H, H5), 2.18 (s, 3H, H10), 1.78 (dd, *J* = 2.8, 14.9 Hz, 1H, H3), 1.6 (dd, *J* = 3.0, 14.9 Hz, 1H, H3), 1.00 (s, 3H, H7/H8), 0.96 (s, 3H, H7/H8). ^{13}C NMR (125 MHz, $CDCl_3$): δ = 210.9 ($Fe(CO)_3$), 170.2 (C9), 128.8 (C1), 76.7 (C6), 65.1 (C5), 58.2 (C2), 43.0 (C3), 34.7 (C4), 34.2 (C7/C8), 30.7 (C7/C8), 21.0 (C9). LR-MS (DIP-MS, 70 eV): *m/z* (%) = 278 (5, $[M - CO]^+$), 250 (15, $[M - 2CO]^+$), 222 (3, $[M - 3CO]^+$), 206 (100), 178 (12), 164 (20), 146 (11), 134 (9), 119 (10), 109 (17), 97 (24), 91 (20), 83 (28), 71 (43), 69 (43), 57 (81), 56 (57, $[Fe]^+$). HR-MS (DIP-MS, 70 eV): *m/z* 278.024 ± 0.0011 (calcd ($[M - CO]^+$): *m/z* 278.0241).

(*RS*)-Tricarbonyl-η^4-(1-acetoxy-5,5-dimethyl-1,3-cyclohexadiene)-iron(0) (*rac*-13). Yield: 525 mg (1.72 mmol, 57%). EA: Calcd for $C_{13}H_{14}FeO_5$: C 51.01; H 4.61. Found: C 50.81; H 4.94. FT-IR (ATR): ν [cm^{-1}] = 2957 (m, C_{sp3}–H), 2860 (w, C_{sp3}–H), 2044 (s, $Fe(CO)_3$), 1962 (bs, $Fe(CO)_3$), 1752 (s, C═O). ^{1}H NMR (500 MHz, $CDCl_3$): δ = 5.40–5.35 (m, 1H, H2), 5.07 (dd, *J* = 4.5, 6.5 Hz, 1H, H3), 2.76 (Ψdd, *J* = 1.0, 6.5 Hz, 1H, H4), 2.20–2.10 (m, 1H, H6), 2.02 (s, 3H, H8), 1.76–1.70 (m, 1H, H6), 1.09 (s, 3H, H9/H10), 0.96 (s, 3H, H9/H10). ^{13}C NMR (125 MHz, $CDCl_3$): δ = 169.7 (C7), 101.9 (C1), 81.3 (C2), 77.4 (C3), 72.6 (C4), 44.9 (C6), 34.9 (C9/C10), 30.9 (C9/C10), 20.9 (C8). LR-MS (DIP-MS, 70 eV): *m/z* (%) = 306 (1, $[M]^+$), 278 (12, $[M - CO]^+$), 250 (36, $[M - 2CO]^+$), 222 (29, $[M - 3CO]^+$), 206 (100), 178 (12), 164 (15), 146 (11), 134 (9), 119 (10), 91 (11), 83 (28), 71 (9), 56 (26, $[Fe]^+$). HR-MS (DIP-MS, 70 eV): *m/z* 278.021 ± 0.0001 (calcd ($[M - CO]^+$): *m/z* 278.0241).

(*RS*)-Tricarbonyl-η⁴-(1-(2,2-dimethylpropanoyloxy)-1,3-cyclohexadiene)iron(0) (*rac*-10). Yield: 895 mg (2.79 mmol, 72%). mp 50.5 °C (from DCM). EA: Calcd for $C_{14}H_{16}FeO_5$: C 52.53; H 5.04. Found: C 52.36; H 5.05. FT-IR (ATR): ν [cm^{-1}] = 2931 (s, C_{sp3}–H), 2859 (m, C_{sp3}–H), 2047 (s, $Fe(CO)_3$), 1970 (bs, $Fe(CO)_3$), 1739 (s, C═O). ^{1}H NMR (500 MHz, $CDCl_3$): δ = 5.39 (d, J = 4.0 Hz, 1H, H2), 5.13 (Ψt, J = 5.5 Hz, 1H, H3), 3.13–3.08 (m, 1H, H4), 2.18–2.09 (m, 1H, H5/H6), 1.92–1.85 (m, 1H, H5/H6), 1.81–1.74 (m, 1H, H5/H6), 1.74–1.64 (m, 1H, H5/H6), 1.22 (s, 9H, H9). ^{13}C NMR (125 MHz, $CDCl_3$): δ = 211.4 ($Fe(CO)_3$), 176.7 (C7), 103.4 (C1), 80.4 (C2/C3), 80.3 (C2/C3), 60.2 (C4), 38.9 (C8), 27.0 (C9), 26.5 (C5/C6), 24.0 (C5/C6). LR-MS (DIP-MS, 70 eV): m/z (%) = 292 (8, $[M - CO]^+$), 264 (49, $[M - 2CO]^+$), 236 (44, $[M - 3CO]^+$), 234 (100), 180 (1), 150 (1), 134 (12), 96 (2), 57 (3, $[C(CH_3)_3]^+$). HR-MS (DIP-MS, 70 eV): m/z 292.040 ± 0.0002 (calcd ($[M - CO]^+$): m/z 292.0398).

(*RS*)-Tricarbonyl-η⁴-(1,3-di-(2,2-dimethylpropanoyloxy)-1,3-cyclohexadiene)iron(0) (*rac*-15). Yield: 899 mg (2.14 mmol, 67%). mp 58.3 °C (from DCM). EA: Calcd for $C_{19}H_{24}FeO_7$: C 54.30; H 5.76. Found: C 54.46; H 5.78. FT-IR (ATR): ν [cm^{-1}] = 2974 (m, C_{sp3}–H), 2926 (m, C_{sp3}–H), 2900 (w, C_{sp3}–H), 2052 (s, $Fe(CO)_3$), 1979 (bs, $Fe(CO)_3$), 1753 (s, C═O), 1740 (s, C═O). ^{1}H NMR (600 MHz, $CDCl_3$): δ = 5.72–5.55 (m, 1H, H2), 3.26–3.25 (m, 1H, H4), 2.12–1.93 (m, 1H, H6), 1.84–1.81 (m, 2H, H5), 1.69–1.62 (m, 1H, H6), 1.23 (s, 9H, H9/H12), 1.17 (s, 9H, H9/H12). ^{13}C NMR (150 MHz, $CDCl_3$): δ = 177.7 (C7/C10), 176.7 (C7/C10), 124.1 (C3), 94.9 (C1), 74.9 (C2), 57.1 (C4), 39.1 (C8/C11), 39.0 (C8/C11), 27.0 (C9/C12), 26.9 (C9/C12), 26.2 (C6), 23.6 (C5). LR-MS (DIP-MS, 70 eV): m/z (%) = 364 (6, $[M - CO]^+$), 336 (40, $[M - 2CO]^+$), 308 (6, $[M - 3CO]^+$), 293 (10), 266 (5), 252 (41), 224 (38), 196 (15), 168 (17), 165 (27), 138 (6), 122 (4), 112 (7), 85 (10), 57 (100), 56 (17, $[Fe]^+$). HR-MS (DIP-MS, 70 eV): m/z 364.097 ± 0.004 (calcd ($[M - CO]^+$): m/z 364.0973).

(*RS*)-Tricarbonyl-η⁴-(1,3-di(2,2-dimethylpropanoyloxy)-5,5-dimethyl-1,3-cyclohexadiene)iron(0) (*rac*-14). Yield: 1.23 g (1.89 mmol, 77%). mp 38.4 °C (from DCM). EA: Calcd for $C_{21}H_{28}FeO_7$: C = 56.26, H = 6.30. Found: C = 56.56, H = 6.26. FT-IR (ATR): ν [cm^{-1}] = 2970 (m, C_{sp3}–H), 2860 (w, C_{sp3}–H), 2050 (s, $Fe(CO)_3$), 1970 (bs, $Fe(CO)_3$), 1742 (s, C═O). ^{1}H NMR (500 MHz, $CDCl_3$): δ = 5.79–5.77 (m, 1H, H2), 3.04 (Ψd, J = 2.2 Hz, 1H, H4), 2.03 (Ψd, J = 14.0 Hz, 1H, H6), 1.64 (Ψd, J = 14.0 Hz, 1H, H6), 1.26 (s, 9H, H11/H14), 1.19 (s, 9H, H11/H14), 1.14 (Ψd, J = 2.9 Hz, 6H, H7, H8). ^{13}C NMR (125 MHz, $CDCl_3$): δ = 210.2 ($Fe(CO)_3$), 177.1 (C9/C12), 176.7 (C9/C12), 122.5 (C3), 93.5 (C1), 76.4 (C2), 69.1 (C4), 44.7 (C6), 39.2 (C10/C13), 39.0 (C10/C13), 35.7 (C5), 34.7(C7/C8), 30.7 (C7/C8), 27.0(C11/C14), 26.9 (C11/C14). LR-MS (DIP-MS, 70 eV): m/z (%) = 420 (1, $[M - CO]^+$), 392 (3, $[M - 2CO]^+$), 364 (34, $[M - 3CO]^+$), 348 (2), 321 (8), 280 (25), 265 (12), 252 (15), 196 (17), 195 (24), 179 (14), 157 (5), 135 (6), 111 (7), 96 (5), 85 (7), 57 (100), 56 (18, $[Fe]^+$). HR-MS (DIP-MS, 70 eV): m/z 392.129 ± 0.0004 (calcd ($[M - 2CO]^+$): m/z 392.1286).

Acknowledgements

This work was supported by the Deutsche Forschungsgemeinschaft (FOR 630) and the Fonds der Chemischen Industrie (doctorate stipend to S.R. and Liebig fellowship to S.A.). We would also like to acknowledge Christoph Schmitz, Philip Christ and Prof. Albrecht Berkessel for technical support concerning the UV/Vis spectroscopic measurements.

Notes and references

1 Special issue: M. K. Choi and L. E. Otterbein ed., *Antioxid. Redox Signal.*, 2002, **4**, 227–338.
2 R. Foresti and R. Motterlini, *Free Radical Res.*, 1999, **31**, 459–475.
3 Review: S. W. Ryter, J. Alam and A. M. K. Choi, *Physiol. Rev.*, 2006, **86**, 583–650.
4 (*a*) Carbon monoxide to prevent lung inflammation, www.clinicaltrials.gov/ct2/show/NCT00094406, accessed 21 March 2012 (*b*) Study of inhaling carbon monoxide to treat patients with intestinal paralysis after colon surgery, www.clinicaltrials.gov/ct2/show/NCT01050712, accessed 21 March 2012.
5 T. R. Johnson, B. E. Mann, J. E. Clark, R. Foresti, C. J. Green and R. Motterlini, *Angew. Chem., Int. Ed.*, 2003, **42**, 3722–3729.
6 R. Motterlini, J. E. Clark, R. Foresti, P. Sarathchandra, B. E. Mann and C. J. Green, *Circ. Res.*, 2002, **90**, e17–e24.
7 P. Naughton, S. Shurey, C. J. Green, T. R. Johnson, B. E. Mann, R. Foresti, R. Motterlini and J. E. Clark, *Circ. Res.*, 2003, **93**, E2–E8.
8 (*a*) R. Motterlini and L. E. Otterbein, *Nat. Rev. Drug Discovery*, 2010, **9**, 728–743; (*b*) B. E. Mann, *Top. Organomet. Chem.*, 2010, **32**, 247–285; (*c*) C. C. Romão, W. A. Blättler, J. D. Seixasa and G. J. L. Bernardesw, *Chem. Soc. Rev.*, 2012, **41**, 3571–3583.
9 Iron-containing CORMs: (*a*) D. Scapens, H. Adams, T. R. Johnson, B. E. Mann, P. Sawle, R. Aqil, T. Perrior and R. Motterlini, *Dalton Trans.*, 2007, 4962–4973; (*b*) I. J. S. Fairlamb, J. M. Lynam, B. E. Moulton, I. E. Taylor, A. K. Duhme-Klair, P. Sawle and R. Motterlini, *Dalton Trans.*, 2007, 3603–3605; (*c*) D. E. Bikiel, E. G. F. Di Salvo, H. M. S. Milagre, M. N. Eberlin, R. S. Correa, J. Ellena, D. A. Estrin and F. Doctorovich, *Inorg. Chem.*, 2011, **50**, 2334–2345; (*d*) L. Hewison, S. H. Crook, T. R. Johnson, B. E. Mann, H. Adams, S. E. Plant, P. Sawle and R. Motterlini, *Dalton Trans.*, 2010, **39**, 8967–8975; (*e*) R. Kretschmer, G. Gessner, H. Görls, S. H. Heinemann and M. Westerhausen, *J. Inorg. Biochem.*, 2011, **105**, 6–9; (*f*) M. A. Gonzalez, N. L. Fry, R. Burt, R. Davda, A. Hobbs and P. K. Mascharak, *Inorg. Chem.*, 2011, **50**, 3127; (*g*) L. Hewison, T. R. Johnson, B. E. Mann, A. J. H. M. Meijer, P. Sawle and R. Motterlini, *Dalton Trans.*, 2011, **40**, 8328–8334; CORMs based on other transition metals: (*h*) A. J. Atkin, S. Williams, P. Sawle, R. Motterlini, J. M. Lynam and I. A. S. Fairlamb, *Dalton Trans.*, 2009, 3653–3656; (*i*) F. Zobi, A. Degonda, M. C. Schnaub and A. Y. Bogonda, *Inorg. Chem.*, 2010, **49**, 7313–7322; (*j*) F. Zobi and O. Blacque, *Dalton Trans.*, 2011, **40**, 4994–5001; (*k*) S. H. Crook, B. E. Mann, A. J. H. M. Meijer, H. Adams, P. D. Scapens and R. Motterlini, *Dalton Trans.*, 2011, **40**, 4230–4235.
10 R. Foresti, M. G. Bani-Hani and R. Motterlini, *Intensive Care Med.*, 2008, **34**, 649–658.
11 R. Motterlini, P. Sawle, J. Hammad, S. Bains, R. Alberto, R. Foresti and C. J. Green, *FASEB J.*, 2005, **19**, 284–286.
12 T. S. Pitchumony, B. Spingler, R. Motterlini and R. Alberto, *Org. Biomol. Chem.*, 2010, **8**, 4849–4854.
13 (*a*) J. Niesel, A. Pinto, H. W. Peindy N'Dongo, K. Merz, I. Ott, R. Gust and U. Schatzschneider, *Chem. Commun.*, 2008, 1798–1800; (*b*) H. Pfeiffer, A. Rojas, J. Niesel and U. Schatzschneider, *Dalton Trans.*, 2009, 4292–4298; (*c*) R. D. Rimmer, H. Richter and P. C. Ford, *Inorg. Chem.*, 2010, **49**, 1180–1185; (*d*) U. Schatzschneider, *Inorg. Chim. Acta*, 2011, **374**, 19–23; (*e*) G. Dördelmann, H. Pfeiffer, A. Birkner and U. Schatzschneider, *Inorg. Chem.*, 2011, **50**, 4362–4367; (*f*) W.-Q. Zhang, A. J. Atkin, I. J. S. Fairlamb, A. C. Whitwood and J. M. Lynam, *Organometallics*, 2011, **30**, 4643–4654; (*g*) R. D. Rimmer, A. E. Pierri and P. C. Ford, *Coord. Chem. Rev.*, 2012, DOI: 10.1016/j.ccr.2011.12.009; (*h*) D. Crespy, K. Landfester, U. S. Schubert and A. Schiller, *Chem. Commun.*, 2010, **46**, 6651–6662.
14 S. Romanski, B. Kraus, U. Schatzschneider, J.-M. Neudörfl, S. Amslinger and H. G. Schmalz, *Angew. Chem., Int. Ed.*, 2011, **50**, 2392–2396.
15 A. Boháč, M. Lettrichová, P. Hrnčiac and M. Hutta, *J. Organomet. Chem.*, 1996, 23–29; A. Boháč, M. Lettrichová and P. Hrnčiac, *Synthesis*, 1991, 881–882.

16 M. E. Flaugh, T. A. Crowell and D. S. Farlow, *J. Org. Chem.*, 1980, **45**, 5399–5400.
17 C. Wawrzénczyk and S. Lochyński, *Monatsh. Chem.*, 1985, **116**, 99–110.
18 Diene 30 could not be obtained without impurities, but complexation of the impure diene led to the desired complex in good yield.
19 M. C. P. Yeh and C.-C. Hwu, *J. Organomet. Chem.*, 1991, **419**, 34–355.
20 I. Teruhiko, U. Eiji, T. Rie and S. Seiki, *J. Org. Chem.*, 2001, **66**, 186–191.
21 For the complexes whose enantiomers could not be separated by GC or HPLC we used both enzymes in the myoglobin assay and used the CO-release as a proof for enzymatic cleavage of the esters, because we did not detect significant CO-release without enzyme for any of the compounds.
22 The presence of a certain amount of oxygen is essential for fast oxidative decomposition, but the Mb-assay does not tolerate high O_2 conditions (reoxidation of the CO-binding Fe(II) in Mb to the non-binding Fe(III)). Additionally, the CO-release rate depends on the concentration of the esterase (enzymatic hydrolysis) and of dithionite (redox potential). To simplify the parameter space we determined the CO-release by GC (O_2 is tolerated and no dithionite is needed). Nevertheless the complexity of the parameter space does not allow a quantitative comparison of the ET-CORMs to those that need different enzymes or to other CORMs. It is also not possible to predict the biological performance, because the enzymes that are used in the lab are not the same as in the living systems.
23 For a comment on the use of $t_{1/2}$ for CORMs, see: A. J. Atkin, J. M. Lynam, B. E. Moulton, P. Sawle, R. Motterlini, N. M. Boyle, M. T. Pryce and I. J. S. Fairlamb, *Dalton Trans.*, 2011, **40**, 5755–5761.
24 The conditions were exactly the same for every complex, except for the use of the enzyme. We classified the prepared complexes into three groups: complexes with the ester at the inner position of the diene (*rac*-**6**, *rac*-**7** and *rac*-**17**), complexes with the ester at the outer position of the diene (*rac*-**8**, *rac*-**10** and *rac*-**18**) and diesters (*rac*-**9**, *rac*-**14**, *rac*-**15** and *rac*-**16**). Every group of complexes was treated with the same enzyme (Table 1) to allow a comparison between the complexes.
25 W. K. Alderton, C. E. Cooper and R. G. Knowles, *Biochem. J.*, 2001, **357**, 593–615.
26 H. Kleinert, P. M. Schwarz and U. Förstermann, *Biol. Chem.*, 2005, **384**, 1343–1364.
27 F. Aktan, *Life Sci.*, 2004, **75**, 639–653.
28 (*a*) G. Weiss, G. Werner-Felmayer, E. R. Werner, K. Grünewald, H. Wachter and M. W. Hentze, *J. Exp. Med.*, 1994, **180**, 969–976; (*b*) M. Dlaska and G. Weiss, *J. Immunol.*, 1999, **162**, 6171–6177. Fe^{2+} has also been proven to reduce NO in patients suffering from ACE inhibitor-induced cough: P. Bhalla, N. P. Singh and K. Ravi, *J. Renin–Angiotensin–Aldosterone Syst.*, 2011, **12**, 491–497.
29 H. S. Kim, P. A. Loughran and T. R. Billiar, *Nitric Oxide*, 2008, **18**, 256–265.
30 (*a*) P. Talalay, M. J. De Long and H. J. Prochaska, *Proc. Natl. Acad. Sci. U. S. A.*, 1988, **85**, 8261–8265; (*b*) T. Prestera, W. D. Holtzclaw, Y. Zhang and P. Talalay, *Proc. Natl. Acad. Sci. U. S. A.*, 1993, **90**, 2965–2969; (*c*) A. T. Dinkova-Kostova, W. D. Holtzclaw, R. N. Cole, K. Itoh, N. Wakabayashi, Y. Katoh, M. Yamamoto and P. Talalay, *Proc. Natl. Acad. Sci. U. S. A.*, 2002, **99**, 11908–11913.
31 S. Amslinger, *ChemMedChem*, 2010, **5**, 351–356.
32 (*a*) K. McMillan, D. S. Bredt, D. J. Hirsch, S. H. Snyder, J. E. Clark and B. S. Masters, *Proc. Natl. Acad. Sci. U. S. A.*, 1992, **89**, 11141–11145; (*b*) R. N. Watts, P. Ponka and D. R. Richardson, *Biochem. J.*, 2003, **369**, 429–440.
33 G. M. Sheldrick, *Acta Crystallogr.*, 2008, **A64**, 112–122.
34 A. L. Spek, *Acta Crystallogr.*, 2009, **D65**, 148–155.
35 W. C. Raschke, S. Baird, P. Ralph and I. Nakoinz, *Cell*, 1978, **15**, 261–267.
36 (*a*) B. Kraus and H. Wolff, *Naunyn-Schmiedeberg's. Arch. Pharmacol.*, 2010, **381**, 541–553; (*b*) E. Park, M. R. Quinn, C. E. Wright and G. Schuller-Levis, *J. Leukocyte Biol.*, 1993, **54**, 119–124.